

Extracting Probabilistic Knowledge from Large Language Models for Bayesian Network Parameterization

Aliakbar Nafar¹, Kristen Brent Venable^{2,3}, Zijun Cui¹, Parisa Kordjamshidi¹

¹Michigan State University

²Florida Institute for Human and Machine Cognition (IHMC)

³University of West Florida

{nafarali, cuizijun, kordjams}@msu.edu, bvenable@ihmc.org

Abstract

In this work, we evaluate the potential of Large Language Models (LLMs) in building Bayesian Networks (BNs) by approximating domain expert priors. LLMs have demonstrated potential as factual knowledge bases; however, their capability to generate probabilistic knowledge about real-world events remains understudied. We explore utilizing the probabilistic knowledge inherent in LLMs to derive probability estimates for statements regarding events and their relationships within a BN. Using LLMs in this context allows for the parameterization of BNs, enabling probabilistic modeling within specific domains. Our experiments on eighty publicly available Bayesian Networks, from healthcare to finance, demonstrate that querying LLMs about the conditional probabilities of events provides meaningful results when compared to baselines, including random and uniform distributions, as well as approaches based on next-token generation probabilities. We explore how these LLM-derived distributions can serve as expert priors to refine distributions extracted from data, especially when data is scarce. Overall, this work introduces a promising strategy for automatically constructing Bayesian Networks by combining probabilistic knowledge extracted from LLMs with real-world data. Additionally, we establish the first comprehensive baseline for assessing LLM performance in extracting probabilistic knowledge.

1 Introduction

Bayesian Networks (BNs) are a powerful formalism for representing uncertainty and dependencies between events. The reliability of inference in BNs hinges on the accuracy of the conditional probability table (CPT) entries. CPTs are typically obtained by collecting data (Ji, Xia, and Meng 2015), which can be expensive or unattainable in domains where data is scarce (You, Li, and Shen 2019; Longato et al. 2023). When data is limited, expert judgments are used as priors to be combined with the data for more accurate probability estimation (Mendes 2014). However, experts are often unavailable (Das 2008; Xiaoguang, Yu, and Zhigao 2019); when they are, their competence must be vetted (Hald et al. 2016), and their opinions must be aggregated (McAndrew et al. 2021) before their views can be used. Given these issues, we explore the capability of Large Language Models (LLMs) to act as experts for building BNs.

The potential of language models as sources for extracting factual knowledge has been demonstrated in several stud-

ies (Petroni et al. 2019; Roberts, Raffel, and Shazeer 2020; AlKhamissi et al. 2022; Zhao et al. 2025). However, it remains unclear whether LLMs possess the ability to generate meaningful *probabilistic estimates* for events and their relationships based on their internal knowledge. In this paper, we use the term *probabilistic estimation* to refer to assigning a specific probability to an uncertain proposition by LLM when utilizing its internal knowledge. For instance, consider the question, “What is the probability that a person who smokes cigarettes will develop cancer in their lifetime?” The answer to this question cannot be inferred from the question’s context; however, a medical expert familiar with the literature might approximate 20%. Similarly, we expect an adept language model to produce a similar estimate. This contrasts with providing a *confidence score* for a concrete answer (Xiong et al. 2024) or solving a problem that has a known numerical solution.

We evaluate the probabilistic estimation capabilities of LLMs such as GPT-4o (OpenAI et al. 2024), Gemini Pro 1.5 (Gemini Team et al. 2024), Claude 3.5 (Anthropic 2024), and open-source model DeepSeek-V3 (DeepSeek-AI et al. 2025b) and utilize their internal knowledge to construct domain-specific BNs with **discrete variables**. To provide a detailed analysis and clear evaluation of the parameter estimation, we assume the dependency structure within the BN is given. We note that the dependency structure extraction has been investigated in (Babakov, Reiter, and Bugarín-Diz 2025) and the preliminary results are promising. In our setting, given the structure of a BN, LLMs are required to predict a probability distribution for each node, conditioned on its parent nodes. First, we analyze the quality of the initial distributions estimated by LLMs. Then, we investigate whether they can potentially function as expert-derived prior probabilities. We test this approach, which we denote as Expert-Driven Priors (EDP), by adjusting the LLM predictions with data samples, effectively applying a partial calibration to the model’s initial estimates.

We use LLMs to estimate the CPTs of 80 real-world BNs collected from the literature. Using Kullback–Leibler (KL) divergence (Kullback and Leibler 1951) as our metric, we show that EDP consistently improves LLM’s predictions and offers a higher-quality prior than the conventional uniform baseline, which is employed when no extra information is available. Furthermore, our experiments indicate that

even when the number of data samples is large, incorporating LLM priors improves performance. We further evaluate EDP on BNs used for classification, demonstrating that reducing KL divergence translates into higher downstream classification accuracy. These findings highlight the promise of leveraging LLMs as expert knowledge sources for probabilistic estimation across various real-world domains.

In summary, our contributions are as follows:

- 1) We introduce the first large-scale and comprehensive evaluation of LLM probabilistic estimation with real-world BNs. We investigate differences in LLM accuracy across domains and varying levels of network complexity, highlighting their effectiveness as probabilistic knowledge bases.
- 2) We show that the LLM predicted probabilities can serve as expert-derived priors, and combining them with data improves the estimated probabilities compared to purely data-driven methods or using a uniform prior baseline.
- 3) We evaluate our method on downstream classification tasks and demonstrate that the improved probability distributions lead to higher classification accuracy.
- 4) We introduce an automated procedure for parameterizing real-world BNs given the network structure ¹.

2 Related Work

To the best of our knowledge, this is the first study to use LLMs to parameterize Bayesian networks and to evaluate those parameters against ground-truth probabilities. Most prior work queries LLMs for a single number interpreted as a “confidence” in a class label, which is inherently different from probabilities (Levine 2024). Among the few works that elicit probabilities, evaluation is only done at task accuracy because gold probabilities are unavailable. In contrast, we directly assess the quality of the learned CPTs via KL divergence to the original BN parameters, and in addition, examine downstream classification accuracy.

Probability Estimation. In the most relevant prior work, LLMs are prompted to produce probabilities of binary variables forming shallow BNs with a depth of only two, tailored toward classification tasks (Huang et al. 2025; Feng et al. 2025). Although they show improved downstream classification accuracy, they do not evaluate the full probability distributions because gold probabilities are unavailable. Feng et al. (2025) only evaluates the correctness of the magnitudes of inferred-node probabilities, not having the ground-truth as a basis to evaluate the distributions. By contrast, we obtain a complete probability distribution for every discrete node, including those with more than two states, and evaluate it against real-world BNs of varying depth with known parameters. Further, we show how an improved estimation translates into better downstream classification Tasks. Paruchuri et al. (2024) asks LLMs to calculate the probabilities for a range of values in a given distribution, but their dataset is limited to only 12 questions, and the queries are elementary with no conditional probabilities.

Confidence Elicitation. Confidence elicitation in LLMs has been studied in classification tasks, where a confidence score

ranging from 0 to 1 is assigned to a discrete class label. Among these, Kadavath et al. (2022) treat the models as a white box and use their token probabilities to assess the confidence of a label. But, token likelihood indicates the model’s uncertainty about the next token (Kuhn, Gal, and Farquhar 2023), rather than the confidence of the label. Consequently, Xiong et al. (2024); Yang, Tsai, and Yamada (2024) treat the model as a black-box and use its generated confidence to solve classification datasets. However, confidence is different from probability (Levine 2024) and confidence elicitation does not directly apply to scenarios requiring a probability distribution across multiple states.

Probabilistic Inference. Probabilistic inference is closely related to our task and can be considered a natural extension of probabilistic estimation. Saeed et al. (2021); Nafar, Venable, and Kordjamshidi (2024b) fine-tune BERT-based language models to perform probabilistic inference, while Nafar, Venable, and Kordjamshidi (2024a) utilizes prompt engineering techniques to enable LLMs to conduct probabilistic inference. However, in all these approaches, the explicit probabilities are either provided in the text or learned from the dataset during fine-tuning without any estimation derived from the internal knowledge of language models.

Zero-shot Regression. Our method queries the LLMs for a numeric probability expressed in plain text, in a relatively similar setting to using LLMs for regression. Using LLMs for regression in a zero-shot setting is an emerging field, with a limited number of studies. Following (Vacareanu et al. 2024), which shows that LLMs are capable regressors in a few-shot setting, Nafar, Venable, and Kordjamshidi (2025) tests the regression capability of LLMs in a zero-shot setting (using internal knowledge) for realistic questions such as estimating the medical insurance cost based on age. However, they don’t use any probability estimation.

3 Problem Definition

The main problem addressed in this paper is parameterizing a Bayesian Network given its structure. We formally define the problem as follows, given the structure of a BN $\mathcal{G} = (\mathcal{V}, \mathcal{E})$ where \mathcal{V} is the set of nodes (random variables) and \mathcal{E} is the set of edges (dependencies among variables), the goal is to estimate the parameters, that is, Conditional Probability Tables \mathcal{G}_θ of this network with the help of LLMs. After assigning the parameters, we compare the resulting distribution to ground-truth values of the original BNs.

4 Methodology

As illustrated in Figure 1, our BN-parameterization pipeline has two steps. First, we query an LLM to use its internal probabilistic knowledge to generate probability estimates. Next, we use these estimates in our **Expert-Driven Priors (EDP)** framework, which treats the LLM outputs as priors and refines them with data to produce the final parameters.

Extracting Probabilistic Knowledge

In the first stage of our BN-parameterization pipeline, we use LLMs to acquire probabilistic estimates for every row of the CPTs. Because many nodes are multi-state, asking for a

¹The code and analytical tools are available at <https://github.com/HLR/llm-bn-parameterization>.

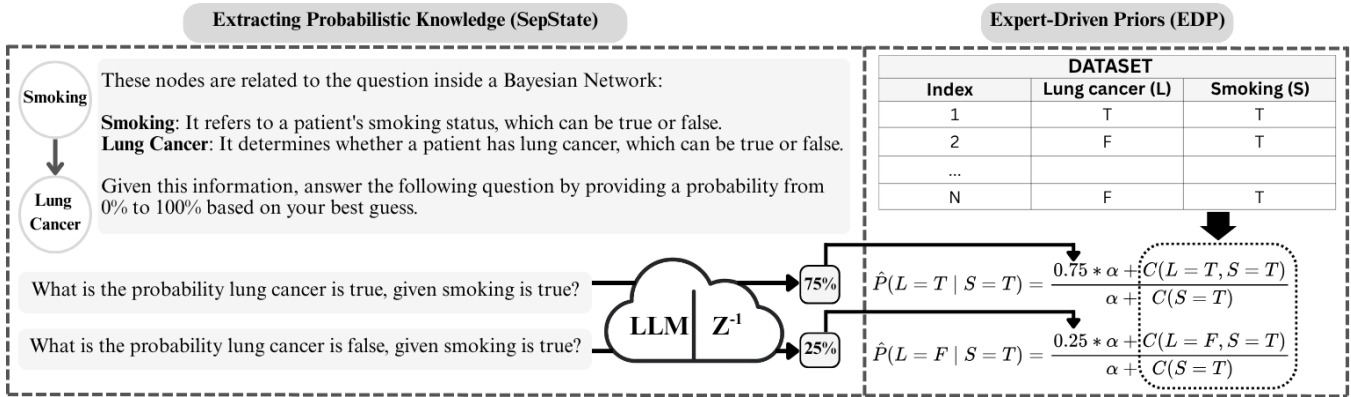


Figure 1: **Two-stage parameterization pipeline.** *SepState (Left Panel):* For each parent configuration, the LLM is prompted with natural-language descriptions of the node and its parents and queried once per state. The answers are subsequently normalized (z^{-1}) into a valid conditional distribution, e.g., (75%, 25%). *EDP (Right Panel):* The LLM-derived prior distribution is translated into pseudocounts and fused with empirical counts (C) to give the posterior estimates. This treats the LLM as a probabilistic expert whose influence is controlled by the hyper-parameter α .

single probability score for each node is impractical. So we use two prompting schemes: **1) FullDist**, where the entire distribution is obtained from the LLM at once in the form of a tuple, e.g., (0.70, 0.20, 0.10). **2) SepState**, where each state is queried independently. Figure 1 depicts the SepState scheme, where the process starts with a prompt template that describes the node and its parents in a natural language format. The descriptions of these nodes, combined with the LLM instructions, are appended to each question presented to the LLM. Each question explicitly defines the states of the node of interest as well as the states of its parent nodes, and poses a probabilistic query based on these assigned states. The LLM is also instructed to articulate its reasoning before generating a probability value. The final answer is extracted as a numerical probability from the output text. Since the raw numeric outputs may not sum to one, they are normalized to form a valid distribution over the node’s states. For a node with m states, the model might produce values p_1, p_2, \dots, p_m that sum to $S = \sum_{i=1}^m p_i$. To convert these values into a valid probability distribution, we divide each one by S . This normalization step can be interpreted as taking the ratio of each state’s assigned likelihood relative to the sum of all states, effectively **preserving the proportions** while enforcing a valid distribution.

FullDist follows the same prompting template, but the LLM is instructed to return the entire distribution in one shot. For example, instead of the two questions in Figure 1, the LLM is asked “What is the probability distribution of lung cancer given that smoking is true?” Thus, the LLM returns a tuple (p_1, \dots, p_m) in a single response. Unlike SepState, the FullDist scheme is concise and requires only one query, independent of the number of the node’s states. However, the autoregressive decoder conditions each number on the previous ones, so early outputs can bias later entries. Concentrating all states in a single prompt could also be too complicated for the LLM. In our experiments, we compare SepState and FullDist schemes empirically.

As noted above, our prompts include brief definitions of

each node and its state space. However, this information can sometimes be extracted from the questions themselves. For example, the meanings of “Lung Cancer” and “Smoking” are commonsense knowledge and known to the LLMs. Also, the LLM can infer that their values are binary, based on the given true/false assignments. However, in cases where the semantic meaning or value sets of nodes are not immediately clear, explicit descriptions are needed. For instance, a node named “X1” must have a clearly stated meaning, such as: “*Represents a lack of supervision and policy guidance, which may lead to the use of unqualified oil. This node can take True or False values.*” Similarly, while the semantic meaning of the “Construction Year” node is self-descriptive, its possible states are ambiguous and need an explanation such as: “*This node indicates the time period in which the building was constructed, with possible values being 1930-1955, 1955-1960, 1960-1968, 1968-1975, and 1975-1980.*” We later test the usage of the contextual descriptions of node meanings and state sets by LLMs in an ablation study to measure their effect on the LLM’s probability predictions.

Expert-Driven Priors (EDP)

Expert opinion and large datasets are either costly or difficult to obtain in many practical scenarios. When only limited data is available, incorporating expert prior knowledge can particularly help offset the shortage of empirical data, thereby improving the estimated probability distributions. We propose that LLMs can approximate these prior distributions based on their knowledge. In our approach, EDP, we combine the LLM-derived probabilities with the empirical distribution estimated from data by using priors as pseudocounts (Zhai and Lafferty 2001).

For a node in the BN with m discrete states, conditioned on a specific parent configuration, the LLM provides a normalized prior distribution q_1, \dots, q_m as shown in the left panel of Figure 1. Then, we use these priors and incorporate data to calculate the final probability distribution. Let c_1, \dots, c_m denote the observed counts listed in the data ta-

ble on the right side of Figure 1. Each prior probability q_i is converted into αq_i virtual observations, where α is a hyperparameter. Larger α values place more weight on the LLM prior, whereas smaller values defer to the data. Adding these pseudocounts to the empirical counts gives the posterior estimate displayed inside the dashed box of Figure 1:

$$p_i = \frac{\alpha q_i + c_i}{\alpha + \sum_{j=1}^m c_j}, \quad i = 1, \dots, m.$$

The numerator combines prior belief (αq_i) with empirical evidence (c_i), while the denominator $\alpha + \sum_j c_j$ normalizes the resulting probabilities. In this manner, we incorporate LLM predictions in the same principled way one would incorporate probabilities elicited from a human expert.

5 Experiments

Dataset of Eighty Bayesian Networks

Our experiments use bnRep (Leonelli 2025), a publicly available collection of BNs spanning diverse domains such as medicine and engineering. These BNs vary in size, ranging from 5 to 50 nodes. Each BN in bnRep has an associated publication detailing its construction, data sources, and domain-specific context. Most of these papers were published recently in the years between 2020 and 2024. Each BN is accompanied by ground-truth parameters, which enable us to evaluate our predictions. We preprocess bnRep to select only discrete BNs and eliminate BNs with missing entries in CPTs, yielding a final dataset of 80 networks. We extract node definitions and states from each BN’s repository paper. Additional details, including preprocessing steps, are provided in Appendix A.

Metrics and Baselines

For LLMs, we use GPT-4o and its mini variant (OpenAI et al. 2024), along with Claude 3.5 Sonnet (Anthropic 2024), Gemini-Pro 1.5 (Gemini Team et al. 2024), and DeepSeek-V3 (DeepSeek-AI et al. 2025b). We include reasoning models, o3 and its mini variant (OpenAI 2025), and DeepSeek-R1 (DeepSeek-AI et al. 2025a). We evaluate the LLM’s estimated BN parameters using Kullback–Leibler (KL) divergence (Kullback and Leibler 1951) compared to ground-truth parameters in bnRep. Specifically, we report the *BN KL divergence*, defined as the KL divergence computed over the BN variables’ joint distribution, evaluating the resulting BN’s overall quality. Refer to Appendix B for an overview of KL divergence, and BN KL divergence, and refer to Appendix C for details on the LLMs and hyperparameters.

We evaluate our methods against multiple baselines. All outputs from these baselines are normalized as necessary to ensure valid probability distributions. These baselines are: (1) **Random** number generator; (2) **Uniform** baseline generating equal probabilities for each row of the CPT, providing basic, uninformed estimations; (3) **LLM (Random)** baseline involving intentionally incorrect queries, where the original variable names are randomly replaced. This is done to assess whether LLMs utilize the content of the provided questions to generate their answers. For instance, we query the LLM “What is the probability that construction time is

true given that lung cancer is true?” instead of the correct question regarding smoking; (4) **LLM (No Context)** baseline in which queries are presented without contextual explanations, exploring scenarios where the node meanings and number of states cannot be directly inferred from the in-context information; (5) **LLM (Token Probability)** baseline, which directly uses the LLM’s internal probabilities assigned to tokens representing node states (e.g., probability of generating the token “True”), rather than explicitly generated numerical probabilities extracted from the model’s textual responses; (6) **MLE-#** is a statistical baseline obtained by maximum likelihood estimation using # data samples; (7) **Uniform-#** applies the same pseudocount updating method as EDP with # data samples, but uses a uniform prior instead of LLM-derived probabilities. Data samples are obtained from the ground-truth BN where the BN is sampled # times using forward sampling. For results obtained using other sampling methods, refer to Appendix D.

Can LLMs Estimate Probabilities Using Their Internal Knowledge?

To evaluate how SepState and FullDist compare to other baseline models, we analyze the distributions of *BN KL divergence* across all 80 BNs, as depicted in Figure 2. The worst-performing models, which perform worse than random, are the “Token Probability” models, shown with yellow boxes. This aligns with previous research, which found that raw token probabilities from LLMs alone are insufficient for effective uncertainty/probability estimation (Xiong et al. 2024) and require additional processing steps like fine-tuning (Tao et al. 2024). The next weakest results are observed among the random generators, alongside the baselines that do not receive the context of nodes and their states. In our experiments, LLM (Random) models slightly surpass the outputs of the Random number generator baseline. However, these improvements only reflect the non-uniformity of random number generation by LLMs, influenced by factors such as text-generation sampling methods and model architecture choices (Hopkins, Renda, and Carbin 2023). Of all the baseline models, the uniform predictor performs best. This result aligns with information theory, which suggests that, in the absence of knowledge, a uniform distribution naturally provides the lowest KL divergence based on uncertainty (Cover and Thomas 2006).

Both FullDist and SepState outperform the uniform baseline in all non-reasoning models. o3 and DeepSeek-R1 trail their non-reasoning counterparts, hinting that high levels of reasoning do not translate to better probabilistic estimation. While the FullDist yields informed estimates, it consistently falls short of SepState with a higher median KL divergence and a greater standard deviation, except in the DeepSeek model. These results confirm the shortcomings of the FullDist scheme and establish SepState as a superior method to extract a full probability distribution from LLMs. Overall, these results demonstrate the capability of LLMs to provide meaningful probability distributions, laying the groundwork for treating them as informative priors in EDP.

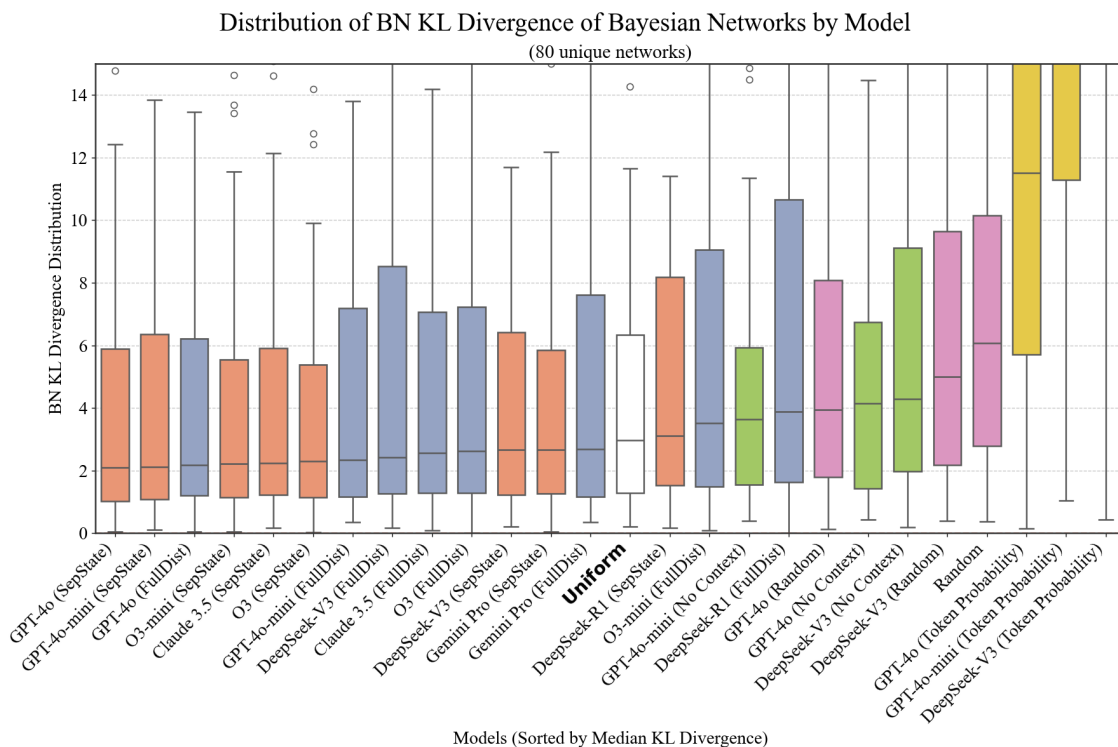


Figure 2: Boxplot showing the distribution of BN KL divergence values across 80 unique BNs for various models, sorted by their median KL divergence. Lower values indicate better alignment with ground truth CPTs.

Can LLMs’ Probability Distribution Estimates Serve as Expert Priors?

In this section, we evaluate the effectiveness of EDP, which combines the LLM-derived distributions with empirical data, using priors as pseudocounts. Figure 3 displays the distributions of BN KL divergences obtained by combining various sample sizes of data with GPT-4o priors (EDP-#) and Uniform priors (Uniform-#). The Uniform prior is the conventional choice in the absence of prior information and serves as a baseline prior in our experiments.

EDP predictions consistently outperform the Uniform-# baseline, proving its use as a better prior. The advantage of EDP is most notable at smaller sample sizes, i.e., 3 to 30 samples. The combination of even minimal data in EDP significantly outperforms SepState and the MLE model with 30 data samples. Additionally, EDP still improves the median KL divergence when more data are available, e.g., 1,000 samples. It also effectively reduces the standard deviation of the predictions, enhancing model robustness. This improvement in median KL divergence at large sample sizes occurs because nodes with unlikely parent combinations rarely receive data. When data are sufficiently large, such as 10k samples in our setting, MLE achieves the best KL divergence, as expected. However, this outcome relies on our forward sampling procedure, which ensures every node of the BN is sampled. In the real world, data are often sparse or biased. In this case, even with 10k samples, EDP can still provide benefits, as we will show in the next section.

For brevity, the main text reports EDP results only for GPT-4o. The corresponding EDP plots for every other LLM priors that outperforms the Uniform baseline in Figure 2 display the exact same pattern as EDP with GPT-4o and are included in Appendix D. These findings confirm that incorporating LLM predictions as expert-driven priors is beneficial and enhances the performance and robustness of parameter estimation in Bayesian Networks.

What Is EDP’s Impact on Downstream Tasks?

We have shown that EDP lowers BN KL divergence, but this alone does not guarantee better performance on downstream tasks. To test whether improved probability estimates translate into downstream gains, we focus on classification, one of the most common BN applications. Following the experimental setting of (Carli et al. 2022), we select nine real-world datasets that are routinely used for BN-based classification studies, each with one target random variable. Every dataset is stratified into 80% training and 20% test splits. For each dataset, two BN structures are used: (i) a structure discovered via Hill Climbing, learned based on the full training data, and (ii) a simpler Naïve Bayes structure. Besides the full-data regime, we simulate low-resource scenarios by using the same network structure but restricting the training set to 20 and 10 samples for parameter estimation, and averaging the results over 5 random runs. We evaluate two LLMs, GPT-4o and DeepSeek-V3, using Chain-of-Thought (COT) (Wei et al. 2022), SepState, MLE, and EDP.

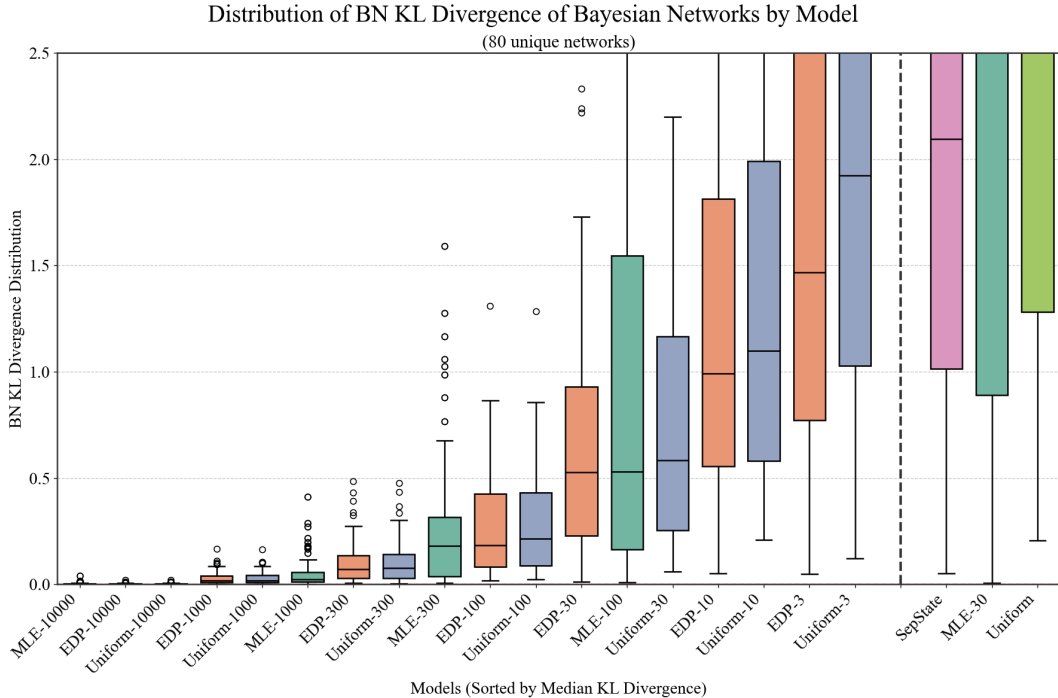


Figure 3: Boxplot of distribution of BN KL divergence over 80 networks, contrasting models with GPT-4o priors (EDP-#), uniform priors (Uniform-#), and data-only estimates (MLE-#). The numeral after the “-” denotes the sample size.

Table 1 reports macro F_1 scores of these methods over 9 datasets and compares them for each network structure. EDP improves over pure data fitting (MLE), especially when data are scarce. The advantage of EDP is most evident in the derived structure from Hill Climbing because learning parameters for its complex structure is more difficult with scarce data. With full training sets, EDP still edges out or ties MLE in 12 out of 18 cases, which confirms the language models can help reduce the bias caused by sampled data. The only notable dip appears in HouseVotes84 and puffin, two datasets whose full-data MLE classifiers already touch the optimal ceiling (0.94–1.00). Even then, EDP does not significantly harm performance.

The trend holds when switching from a Hill Climbing structure to Naïve Bayes, and EDP surpasses MLE at every data size. This trend also remains consistent when we test DeepSeek-V3 (tables are moved to Appendix D for space). The only difference is that we get better classification results with EDP using the FullDist scheme for DeepSeek-V3, which achieved a better parameter estimation based on the obtained KL divergence as shown in Figure 2. Taken together, these findings corroborate the central claim that LLM-derived probability estimates are not only closer to ground truth compared to other alternative baselines but are also effective in downstream tasks.

6 Discussion

Quality of Individual Distributions Versus the Entire BN. In our experiments, we used the BN KL divergence metric to

evaluate the quality of the predicted BNs parameters. However, this metric assesses the entire BN, meaning that a few poorly predicted nodes might disproportionately influence the evaluation. To address this limitation, we also analyzed the *CPT KL Divergence*, which computes the average KL divergence across all individual CPT rows within each BN. This alternative measure evaluates the quality of individual distributions rather than the BN as a whole. Using CPT KL Divergence, we observed that the overall trends of our results remained consistent. Additional diagrams illustrating these findings are provided in Appendix D.

Performance Variations Among LLMs Across Different BN Domains. Among the evaluated LLMs, GPT-4o consistently exceeds the performance of other LLMs, though specific models perform better within specialized domains. For instance, Claude 3.5, Gemini-pro, and GPT-4o achieve the best results on BNs related to engineering, business, and medical domains, respectively. Furthermore, there are inherent differences in prediction behavior among these LLMs, likely attributed to their respective training methodologies. Specifically, Claude 3.5 performed best on BNs with low entropy probabilities, but showed the poorest performance on BNs with high entropy probabilities among the LLMs, indicating an overly confident prediction behavior. In contrast, Gemini-pro showed the opposite trend, whereas GPT-4o had a more balanced prediction profile.

Handling Larger Parent Sets and States. Intuitively, it is expected that LLMs may struggle to provide informed predictions for more complex queries involving nodes with

Dataset	Size	Baseline			Hill Climbing						Naïve Bayes						
		Random	COT	SepState	Full Data		20 Samples		10 Samples		SepState	Full Data		20 Samples		10 Samples	
					MLE	EDP	MLE	EDP	MLE	EDP		MLE	EDP	MLE	EDP	MLE	EDP
HouseVotes84	435	0.52	0.50	0.24	0.94	0.91	0.87	0.80	0.78	0.85	0.40	0.94	0.91	0.92	0.90	0.91	0.87
PhDArticles	915	0.38	0.39	0.41	0.38	0.41	0.35	0.41	0.34	0.41	0.45	0.44	0.44	0.36	0.41	0.34	0.41
Pokemon	999	0.50	0.43	0.23	0.62	0.62	0.62	0.62	0.54	0.54	0.48	0.62	0.60	0.59	0.60	0.53	0.54
Titanic	32	0.51	0.71	0.42	0.42	0.42	0.42	0.42	0.42	0.42	0.57	0.11	0.55	0.22	0.57	0.42	0.56
CAD1	236	0.54	0.55	0.87	0.83	0.83	0.74	0.85	0.63	0.84	0.77	0.81	0.85	0.83	0.86	0.80	0.84
CAD2	67	0.44	0.44	0.76	0.65	0.76	0.76	0.76	0.60	0.76	0.50	0.86	0.79	0.73	0.78	0.77	0.78
Covid	10k	0.54	0.64	0.74	0.71	0.73	0.70	0.72	0.72	0.72	0.72	0.71	0.72	0.71	0.72	0.69	0.72
Puffin	69	0.50	0.43	0.63	1.00	0.93	0.99	0.91	0.97	0.91	0.78	0.93	0.85	0.90	0.88	0.87	0.88
Trajectories	10k	0.59	0.78	0.87	0.87	0.87	0.75	0.86	0.68	0.86	0.80	0.87	0.87	0.86	0.86	0.85	0.86
Average	-	0.50	0.54	0.57	0.71	0.72	0.69	0.71	0.63	0.70	0.61	0.70	0.73	0.68	0.73	0.69	0.72

Table 1: Macro- F_1 classification scores on nine datasets for BN classifiers. Columns include three methods, *SepState* using GPT-4o, *MLE*, and *EDP*, under two graph structures, HillClimbing and Naïve Bayes. Full Data uses the entire training split, whereas 20 and 10 Samples simulate low-resource regimes. Within each data regime, the higher of *MLE* vs. *EDP* is bolded.

many parent nodes or states. We use the CPT KL Divergence metric to assess predictions among these nodes, which averages the KL divergence across all individual CPT rows rather than evaluating the entire BN. In our experiments with realistic BNs, LLM performance in these scenarios still surpassed our baseline models. LLMs consistently outperformed baselines in queries involving up to 5 parent nodes. Additionally, the LLMs performed better than baselines for nodes with 2 or 3 states. Nodes exceeding 3 states are rare in realistic BNs. Only 4 BNs had nodes restricted to 4 states, whereas 11 featured nodes with 5 states. Within these BNs, except for the 'DustExplosion' BN, the LLMs consistently outperformed baseline methods. 'DustExplosion' contained nodes with both 4 and 5 states and is designed to predict explosion probabilities in industrial environments, which proved challenging for the LLMs. For detailed results demonstrating the performance with varying numbers of parent nodes and states, refer to Appendix E.

Trade-off Between SepState and FullDist Schemes. Our experiments show that SepState consistently outperforms FullDist, in 7 out of 8 models, achieving lower median KL divergence and improved stability. Although the FullDist scheme is more straightforward and requires fewer queries, it leads to less precise and more variable estimates. Thus, we recommend SepState for applications prioritizing accuracy and consistency, while FullDist might be suitable in scenarios where cost saving is paramount.

EDP's Application for Automated BN Construction. The demonstrated capability of LLMs, particularly GPT-4o, in the EDP method has significant implications for automating BN construction. Traditionally, parameterization of BNs relies heavily on expert input, making the process labor-intensive, costly, and dependent on the availability of reliable experts. Utilizing an LLM proficient across diverse domains removes these barriers and holds enormous potential for advancing automation in BN parameterization.

EDP with Small Data for Extraction of Probabilistic Knowledge. We showed the potential of using LLM predictions in place of expert-driven priors for constructing

BNs. As shown in Figure 3, EDP with just a few data samples, such as 3, yields a lower BN KL divergence than both MLE trained on more data, like MLE-30, or the LLM-only (SepState). These results highlight a promising application wherein LLMs use minimal external data points to rapidly refine their predictions for probabilistic queries. Such a small amount of data could be supplied to the LLM in various ways, such as being obtained online by querying information from publicly available sources (e.g., occurrences of lung cancer among smokers). EDP not only improves data efficiency and outperforms uniform baseline methods but also provides an exciting possibility for real-time improvement of LLM-generated probabilistic estimates with minimal data input.

7 Conclusion and Future Work

In this work, we demonstrate that modern LLMs can effectively produce conditional probabilities to be used as expert-driven priors for Bayesian Networks parameterization. EDP proved superior to the approach of using Uniform priors and purely data-driven approaches, especially in a low-data regime. Furthermore, we show that employing EDP to estimate parameters of the BNs improved the accuracy in downstream tasks. In conclusion, this study introduces a novel pipeline for parameterizing BNs using LLMs. Using LLMs as a resource compensates for the lack of data and reduces the need for costly domain experts. We also establish the first comprehensive framework for evaluating the probabilistic knowledge of LLMs with real-world probabilistic BNs.

Future work will focus on advancing toward a fully automated framework for BN construction. In this regard, the key challenge lies in automating the structure learning component. Although preliminary efforts have been made in this area, there is significant potential to create an end-to-end pipeline using LLMs that generates a BN structure, parameterizes it, and systematically evaluates its performance.

References

- AlKhamissi, B.; Li, M.; Celikyilmaz, A.; Diab, M.; and Ghazvininejad, M. 2022. A Review on Language Models as Knowledge Bases. arXiv:2204.06031.
- Ankan, A.; and Panda, A. 2015. pgmpy: Probabilistic graphical models using python. In *Proceedings of the 14th Python in Science Conference (SCIPY 2015)*. Citeseer.
- Anthropic. 2024. Claude 3.5 Sonnet. Large language model. Accessed: 21 Feb. 2025.
- Babakov, N.; Reiter, E.; and Bugarín-Diz, A. 2025. Scalability of Bayesian Network Structure Elicitation with Large Language Models: a Novel Methodology and Comparative Analysis. In Rambow, O.; Wanner, L.; Apidianaki, M.; Al-Khalifa, H.; Eugenio, B. D.; and Schockaert, S., eds., *Proceedings of the 31st International Conference on Computational Linguistics*, 10685–10711. Abu Dhabi, UAE: Association for Computational Linguistics.
- Carli, F.; Leonelli, M.; Riccomagno, E.; and Varando, G. 2022. The R Package stagedtrees for Structural Learning of Stratified Staged Trees. *Journal of Statistical Software*, 102(6): 1–30.
- Chase, H. 2022. LangChain.
- Cover, T. M.; and Thomas, J. A. 2006. *Elements of Information Theory (Wiley Series in Telecommunications and Signal Processing)*. USA: Wiley-Interscience. ISBN 0471241954.
- Das, B. 2008. Generating Conditional Probabilities for Bayesian Networks: Easing the Knowledge Acquisition Problem. arXiv:cs/0411034.
- DeepSeek-AI; Guo, D.; Yang, D.; Zhang, H.; Song, J.; et al. 2025a. DeepSeek-R1: Incentivizing Reasoning Capability in LLMs via Reinforcement Learning. arXiv:2501.12948.
- DeepSeek-AI; Liu, A.; Feng, B.; Xue, B.; et al. 2025b. DeepSeek-V3 Technical Report. arXiv:2412.19437.
- Feng, Y.; Zhou, B.; Lin, W.; and Roth, D. 2025. BIRD: A Trustworthy Bayesian Inference Framework for Large Language Models. In *The Thirteenth International Conference on Learning Representations*.
- Gemini Team; et al. 2024. Gemini: A Family of Highly Capable Multimodal Models. arXiv:2312.11805.
- Hald, T.; Aspinall, W.; Devleeschauwer, B.; Cooke, R.; Corrigan, T.; Havelaar, A. H.; Gibb, H. J.; Torgerson, P. R.; Kirk, M. D.; Angulo, F. J.; Lake, R. J.; Speybroeck, N.; and Hoffmann, S. 2016. World Health Organization Estimates of the Relative Contributions of Food to the Burden of Disease Due to Selected Foodborne Hazards: A Structured Expert Elicitation. *PLOS ONE*, 11(1): 1–35.
- Hopkins, A. K.; Renda, A.; and Carbin, M. 2023. Can LLMs Generate Random Numbers? Evaluating LLM Sampling in Controlled Domains. In *ICML 2023 Workshop: Sampling and Optimization in Discrete Space*.
- Huang, H.; Shen, X.; Wang, S.; Meng, L.; Liu, D.; Wang, H.; and Bhatt, S. 2025. Verbalized Probabilistic Graphical Modeling. arXiv:2406.05516.
- Ji, Z.; Xia, Q.; and Meng, G. 2015. A Review of Parameter Learning Methods in Bayesian Network. In Huang, D.-S.; and Han, K., eds., *Advanced Intelligent Computing Theories and Applications*, 3–12. Cham: Springer International Publishing. ISBN 978-3-319-22053-6.
- Kadavath, S.; Conerly, T.; Askell, A.; Henighan, T.; Drain, D.; Perez, E.; Schiefer, N.; Hatfield-Dodds, Z.; DasSarma, N.; Tran-Johnson, E.; Johnston, S.; El-Showk, S.; Jones, A.; Elhage, N.; Hume, T.; Chen, A.; Bai, Y.; Bowman, S.; Fort, S.; Ganguli, D.; Hernandez, D.; Jacobson, J.; Kernion, J.; Kravec, S.; Lovitt, L.; Ndousse, K.; Olsson, C.; Ringer, S.; Amodei, D.; Brown, T.; Clark, J.; Joseph, N.; Mann, B.; McCandlish, S.; Olah, C.; and Kaplan, J. 2022. Language Models (Mostly) Know What They Know. arXiv:2207.05221.
- Kuhn, L.; Gal, Y.; and Farquhar, S. 2023. Semantic Uncertainty: Linguistic Invariances for Uncertainty Estimation in Natural Language Generation. arXiv:2302.09664.
- Kullback, S.; and Leibler, R. A. 1951. On Information and Sufficiency. *The Annals of Mathematical Statistics*, 22(1): 79–86.
- Leonelli, M. 2025. bnRep: A repository of Bayesian networks from the academic literature. *Neurocomputing*, 624: 129502.
- Levine, R. 2024. Probability or confidence, a distinction without a difference? *Intelligence and National Security*, 39(4): 729–741.
- Longato, E.; Tavazzi, E.; Chió, A.; Mora, G.; Sparacino, G.; and Di Camillo, B. 2023. Dealing with Data Scarcity in Rare Diseases: Dynamic Bayesian Networks and Transfer Learning to Develop Prognostic Models of Amyotrophic Lateral Sclerosis. In Juarez, J. M.; Marcos, M.; Stiglic, G.; and Tucker, A., eds., *Artificial Intelligence in Medicine*, 140–150. Cham: Springer Nature Switzerland. ISBN 978-3-031-34344-5.
- McAndrew, T.; Wattanachit, N.; Gibson, G. C.; and Reich, N. G. 2021. Aggregating predictions from experts: A review of statistical methods, experiments, and applications. *Wiley Interdisciplinary Reviews: Computational Statistics*, 13(2): e1514. Epub 2020 Jun 16.
- Mendes, E. 2014. *Expert-Based Knowledge Engineering of Bayesian Networks*, 73–105. Berlin, Heidelberg: Springer Berlin Heidelberg. ISBN 978-3-642-54157-5.
- Nafar, A.; Venable, K. B.; and Kordjamshidi, P. 2024a. Reasoning over Uncertain Text by Generative Large Language Models. arXiv:2402.09614.
- Nafar, A.; Venable, K. B.; and Kordjamshidi, P. 2024b. Teaching Probabilistic Logical Reasoning to Transformers. In Graham, Y.; and Purver, M., eds., *Findings of the Association for Computational Linguistics: EACL 2024*, 1615–1632. St. Julian’s, Malta: Association for Computational Linguistics.
- Nafar, A.; Venable, K. B.; and Kordjamshidi, P. 2025. Learning vs Retrieval: The Role of In-Context Examples in Regression with Large Language Models. arXiv:2409.04318.
- OpenAI. 2025. OpenAI o3 and o4-mini System Card. <https://openai.com/index/o3-o4-mini-system-card>. System card describing the architecture, training, and evaluations of the o3 reasoning model.

- OpenAI; et al. 2024. GPT-4o System Card. *arXiv:2410.21276*.
- Paruchuri, A.; Garrison, J.; Liao, S.; Hernandez, J. B.; Sunshine, J.; Althoff, T.; Liu, X.; and McDuff, D. 2024. What Are the Odds? Language Models Are Capable of Probabilistic Reasoning. In Al-Onaizan, Y.; Bansal, M.; and Chen, Y.-N., eds., *Proceedings of the 2024 Conference on Empirical Methods in Natural Language Processing*, 11712–11733. Miami, Florida, USA: Association for Computational Linguistics.
- Petroni, F.; Rocktäschel, T.; Riedel, S.; Lewis, P.; Bakhtin, A.; Wu, Y.; and Miller, A. 2019. Language Models as Knowledge Bases? In Inui, K.; Jiang, J.; Ng, V.; and Wan, X., eds., *Proceedings of the 2019 Conference on Empirical Methods in Natural Language Processing and the 9th International Joint Conference on Natural Language Processing (EMNLP-IJCNLP)*, 2463–2473. Hong Kong, China: Association for Computational Linguistics.
- Roberts, A.; Raffel, C.; and Shazeer, N. 2020. How Much Knowledge Can You Pack Into the Parameters of a Language Model? In Webber, B.; Cohn, T.; He, Y.; and Liu, Y., eds., *Proceedings of the 2020 Conference on Empirical Methods in Natural Language Processing (EMNLP)*, 5418–5426. Online: Association for Computational Linguistics.
- Saeed, M.; Ahmadi, N.; Nakov, P.; and Papotti, P. 2021. RuleBERT: Teaching Soft Rules to Pre-Trained Language Models. In Moens, M.-F.; Huang, X.; Specia, L.; and Yih, S. W.-t., eds., *Proceedings of the 2021 Conference on Empirical Methods in Natural Language Processing*, 1460–1476. Online and Punta Cana, Dominican Republic: Association for Computational Linguistics.
- Tao, S.; Yao, L.; Ding, H.; Xie, Y.; Cao, Q.; Sun, F.; Gao, J.; Shen, H.; and Ding, B. 2024. When to Trust LLMs: Aligning Confidence with Response Quality. In Ku, L.-W.; Martins, A.; and Srikumar, V., eds., *Findings of the Association for Computational Linguistics: ACL 2024*, 5984–5996. Bangkok, Thailand: Association for Computational Linguistics.
- Vacareanu, R.; Negru, V. A.; Suci, V.; and Surdeanu, M. 2024. From Words to Numbers: Your Large Language Model Is Secretly A Capable Regressor When Given In-Context Examples. In *First Conference on Language Modeling*.
- Wei, J.; Wang, X.; Schuurmans, D.; Bosma, M.; Ichter, B.; Xia, F.; Chi, E.; Le, Q. V.; and Zhou, D. 2022. Chain-of-Thought Prompting Elicits Reasoning in Large Language Models. In Koyejo, S.; Mohamed, S.; Agarwal, A.; Belgrave, D.; Cho, K.; and Oh, A., eds., *Advances in Neural Information Processing Systems*, volume 35, 24824–24837. Curran Associates, Inc.
- Xiaoguang, G.; Yu, Y.; and Zhigao, G. 2019. Learning Bayesian networks by constrained Bayesian estimation. *Journal of Systems Engineering and Electronics*, 30(3): 511–524.
- Xiong, M.; Hu, Z.; Lu, X.; LI, Y.; Fu, J.; He, J.; and Hooi, B. 2024. Can LLMs Express Their Uncertainty? An Empirical Evaluation of Confidence Elicitation in LLMs. In *The Twelfth International Conference on Learning Representations*.
- Yang, D.; Tsai, Y.-H. H.; and Yamada, M. 2024. On Verbalized Confidence Scores for LLMs. *arXiv preprint arXiv:2412.14737*.
- You, Y.; Li, J.; and Shen, L. 2019. An effective Bayesian network parameters learning algorithm for autonomous mission decision-making under scarce data. *International Journal of Machine Learning and Cybernetics*, 10: 549–561.
- Zhai, C.; and Lafferty, J. 2001. A study of smoothing methods for language models applied to Ad Hoc information retrieval. In *Proceedings of the 24th Annual International ACM SIGIR Conference on Research and Development in Information Retrieval, SIGIR '01*, 334–342. New York, NY, USA: Association for Computing Machinery. ISBN 1581133316.
- Zhao, W. X.; Zhou, K.; Li, J.; Tang, T.; Wang, X.; Hou, Y.; Min, Y.; Zhang, B.; Zhang, J.; Dong, Z.; Du, Y.; Yang, C.; Chen, Y.; Chen, Z.; Jiang, J.; Ren, R.; Li, Y.; Tang, X.; Liu, Z.; Liu, P.; Nie, J.-Y.; and Wen, J.-R. 2025. A Survey of Large Language Models. *arXiv:2303.18223*.

A Dataset Pre-processing

bnRep Dataset Overview

The bnRep dataset (Leonelli 2025) is an open-source collection designed to facilitate research, teaching, and practical applications related to Bayesian Networks (BNs), addressing the significant shortage of comprehensive BN repositories. Implemented as an R package, bnRep includes over 200 well-documented Bayesian Networks sourced from more than 150 academic publications, mainly recent studies published from 2020 onwards. Each BN entry has accompanying characteristics extracted from the original publications. These characteristics are described below:

- **Name:** A short identifier for the Bayesian network.
- **Type:** The network’s type of random variables (discrete, continuous, mixture).
- **Structure:** Indicates how the network’s structure was obtained.
 - *Knowledge:* The structure is built from well-established domain knowledge.
 - *Data:* The structure was learned from a dataset.
 - *Fixed:* A predefined structure that is neither purely elicited from experts nor learned from data (often a canonical or standard network).
 - *Synthetic:* The structure was generated artificially (e.g., for algorithm testing).
 - *Expert:* The structure is directly elicited from domain experts.
 - *Mixed:* The structure is derived through a combination of sources.
- **Probabilities:** Indicates how the CPTs were obtained:
 - *Data:* Parameters estimated from empirical data.
 - *Knowledge:* Parameters derived from well-established theoretical or domain-specific information.
 - *Mixed:* A combination of data-based estimation and expert input.
 - *Synthetic:* Artificially generated parameters for testing or demonstration.
 - *Expert:* Parameters directly elicited from domain experts.
- **Graph:** Describes any special structural characteristic of the network graph. For example:
 - *Generic:* No particular restriction or canonical form.
 - *Naive Bayes:* A star-shaped structure often used for classification tasks.
 - *Reverse Naive Bayes:* The class label is modeled as a child of all other variables, reversing the direction of edges in the standard Naive Bayes structure.
 - *K-Dep:* Each feature depends on the class and up to K other features.
 - *Tree:* A graph with each node having exactly one parent (except the root).
 - *Reverse Tree:* A tree with reversed edges, placing the class node at the leaves.

- *TAN:* an extension of Naive Bayes that allows each variable to have one additional parent, forming a tree among the predictors for greater flexibility.

- **Area:** The domain of the BN (e.g., Medicine, Engineering, Environmental Science).
- **Nodes:** The total number of random variables (nodes) in the Bayesian network.
- **Arcs:** The total number of directed edges (arcs) in the network.
- **Parameters:** The total number of probability entries in the CPTs.
- **Avg. Parents:** The average number of parent nodes per variable.
- **Max Parents:** The maximum number of parents any single node has in the network.
- **Avg. Levels:** The average number of discrete states (levels) per node.
- **Max Levels:** The maximum number of states among all nodes in the network.
- **Average Markov Blanket:** The average size of the Markov blanket for each node, which consists of the node’s parents, children, and the children’s other parents.
- **Year:** The year of publication associated with the BN’s reference.
- **Journal:** The venue where the Bayesian network was published or described.
- **Reference:** The bibliographic reference describing the BN in detail.

BN Selection and Filtering

To utilize the bnRep dataset, we first converted the Bayesian Networks from the R package into Python-compatible format using the pgmpy library (Ankan and Panda 2015). Next, we filtered the networks, selecting only those containing discrete CPT values, as these comprise the majority of the BNs. Then, to improve practicality and computational efficiency, we excluded networks with more than 50 nodes due to practical and cost considerations, noting that only a few exceed this threshold. The most substantial reduction, however, came from removing BNs with incomplete CPT information. After applying all these criteria, we arrived at a final dataset of 80 BNs, which remains sufficiently large for our evaluation purposes.

Nodes’ Descriptions and States

Querying the LLMs for each node requires clearly defined descriptions for the nodes and their respective states. To acquire this information for each BN, we first retrieved the PDFs of the referenced documents that detail each BN. These references were initially provided by the bnRep dataset. A Python script was developed to automate the download of relevant PDFs directly from Google Scholar using bibliographic information. Despite automation, several documents could not be downloaded automatically due to access restrictions or other limitations. As a result, these remaining documents were obtained manually. Subsequently,

we performed a manual verification to ensure the documents corresponded to their respective references.

We then implemented another Python script leveraging GPT-4o, which, given a PDF and the extracted nodes and states of the Bayesian Network (obtained through the pgmpy library), automatically generated a Python dictionary describing each node and its associated states. The majority of generated dictionaries were accurate and required minimal modifications; a few necessitated manual adjustments to ensure correct formatting and accuracy. An illustrative example of the prompt and the generated dictionary for the Bayesian Network “algalactivity2” is provided in Figure 4.

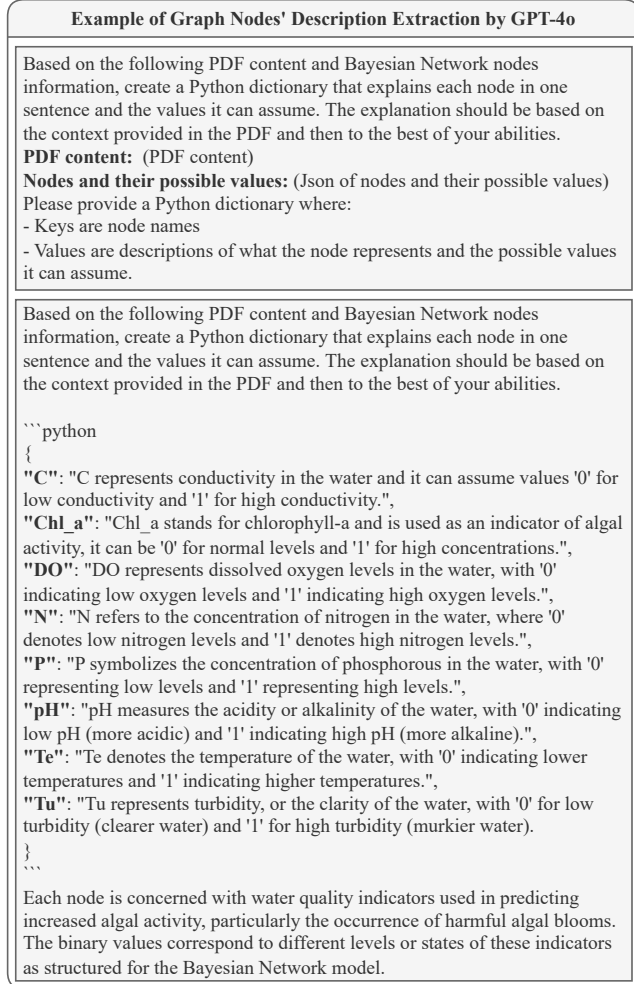


Figure 4: Example of node descriptions and state extractions generated by GPT-4o for the Bayesian Network “algalactivity2”. The Python dictionary describes each node and the possible values it can assume based on context from the provided document.

B KL Divergence

Kullback Leibler (KL) Divergence Overview

Kullback-Leibler (KL) divergence (Kullback and Leibler 1951) measures how one probability distribution p diverges

from a reference distribution q . For a discrete random variable X ,

$$D_{\text{KL}}(p(X) \parallel q(X)) = \sum_{x \in \mathcal{X}} p(x) \log \frac{p(x)}{q(x)}.$$

For continuous variables, the sum is replaced by an integral. KL divergence satisfies $D_{\text{KL}}(p \parallel q) \geq 0$ and equals zero iff $p = q$. It is asymmetric ($D_{\text{KL}}(p \parallel q) \neq D_{\text{KL}}(q \parallel p)$ in general). Intuitively, it quantifies the expected extra amount of information (in nats or bits) required to encode samples from p using a code that is optimal for q . In our implementation, all computations use base-2 logarithms (bits). To avoid undefined terms when $q(x) = 0$ but $p(x) > 0$, we apply elementwise ε -smoothing to both p and q with $\varepsilon = 10^{-8}$:

$$\tilde{r}(x) = \frac{r(x) + \varepsilon}{\sum_{x' \in \mathcal{X}} (r(x') + \varepsilon)} \quad \text{for } r \in \{p, q\},$$

and evaluate $D_{\text{KL}}(\tilde{p} \parallel \tilde{q})$. This guarantees strictly positive probabilities and prevents $\log 0$.

BN KL Divergence Calculation

Calculating the KL divergence over the entire Bayesian network can be computationally expensive. To address this, we decompose it into a weighted sum of CPTs, where the weights correspond to the probabilities of the parent nodes, as illustrated in Figure 5. This approach simplifies computations in practice, since we only need to infer the probabilities of parent nodes using variable elimination.

CPT KL Divergence Calculation

In some of our experiments, we report a CPT KL divergence defined over local CPT rows instead of the entire BN. For each node X_i with parent set pa_i and parent configuration set \mathcal{P}_i , define the local divergence

$$d_{i,u} = D_{\text{KL}}(p(X_i \mid pa_i=u) \parallel q(X_i \mid pa_i=u)), \quad u \in \mathcal{P}_i.$$

Our CPT KL divergence is the unweighted mean over all CPT rows in the BN:

$$\text{CPT KL divergence} = \frac{1}{\sum_{i=1}^n |\mathcal{P}_i|} \sum_{i=1}^n \sum_{u \in \mathcal{P}_i} d_{i,u}.$$

This metric treats every CPT row equally and is therefore suitable for subgroup analyses, e.g., by number of states or by number of parents.

C Setup and Hyper-Parameters

Large Language Models' Versions

In our experiments, we evaluated multiple state-of-the-art Large Language Models: GPT-4o and its mini variant (OpenAI et al. 2024) versions “gpt-4o-2024-11-20” and “gpt-4o-mini-2024-07-18”, Claude 3.5 Sonnet (Anthropic 2024) version “Claude 3.5 Sonnet 2024-10-22”, Gemini-Pro 1.5 (Gemini Team et al. 2024) version “gemini-1.5-pro-002” and DeepSeek-V3 (DeepSeek-AI et al. 2025b), version “DeepSeek-V3-0324”. To test the reasoning models we

BN KL Divergence Decomposition into a Sum of Local KL Divergences

Let $p(\mathbf{x})$ and $q(\mathbf{x})$ be two BNs over the same variables $\{X_1, \dots, X_n\}$ with common structure. Each factorizes as $p(\mathbf{x}) = \prod_{i=1}^n p(x_i | \text{Pa}_i)$, $q(\mathbf{x}) = \prod_{i=1}^n q(x_i | \text{Pa}_i)$, where Pa_i are the parents of X_i . We want to show:

$$D_{\text{KL}}(p \| q) = \sum_{i=1}^n \sum_{\text{pa}_i} p(\text{pa}_i) D_{\text{KL}}(p(X_i | \text{pa}_i) \| q(X_i | \text{pa}_i)).$$

Derivation.

$$\begin{aligned} D_{\text{KL}}(p \| q) &= \sum_{\mathbf{x}} p(\mathbf{x}) \log \frac{p(\mathbf{x})}{q(\mathbf{x})} = \sum_{\mathbf{x}} p(\mathbf{x}) \log \frac{\prod_{i=1}^n p(x_i | \text{Pa}_i)}{\prod_{i=1}^n q(x_i | \text{Pa}_i)} = \sum_{\mathbf{x}} p(\mathbf{x}) \sum_{i=1}^n \log \frac{p(x_i | \text{Pa}_i)}{q(x_i | \text{Pa}_i)} \\ &= \sum_{i=1}^n \sum_{\mathbf{x}} p(\mathbf{x}) \log \frac{p(x_i | \text{Pa}_i)}{q(x_i | \text{Pa}_i)} = \sum_{i=1}^n \sum_{\text{pa}_i} p(\text{pa}_i) \sum_{x_i} p(x_i | \text{pa}_i) \log \frac{p(x_i | \text{pa}_i)}{q(x_i | \text{pa}_i)} \\ &= \sum_{i=1}^n \sum_{\text{pa}_i} p(\text{pa}_i) D_{\text{KL}}(p(X_i | \text{pa}_i) \| q(X_i | \text{pa}_i)). \end{aligned}$$

Example. Let $A, B, C \in \{0, 1\}$ within the network $A \rightarrow B \rightarrow C$. We compute $D_{\text{KL}}(p \| q)$ as follows:

1. **Substitute the factorizations:**

$$D_{\text{KL}}(p \| q) = \sum_{a,b,c} p(a, b, c) \log \frac{p(a, b, c)}{q(a, b, c)} = \sum_{a,b,c} p(a, b, c) \log \frac{p(a) p(b | a) p(c | b)}{q(a) q(b | a) q(c | b)}.$$

2. **Separate logs:**

$$= \sum_{a,b,c} p(a, b, c) \left[\log \frac{p(a)}{q(a)} + \log \frac{p(b | a)}{q(b | a)} + \log \frac{p(c | b)}{q(c | b)} \right].$$

3. **Split the sum:**

$$= \underbrace{\sum_{a,b,c} p(a, b, c) \log \frac{p(a)}{q(a)}}_A + \underbrace{\sum_{a,b,c} p(a, b, c) \log \frac{p(b | a)}{q(b | a)}}_B + \underbrace{\sum_{a,b,c} p(a, b, c) \log \frac{p(c | b)}{q(c | b)}}_C.$$

4. **Marginalize:**

$$A = \sum_a p(a) \log \frac{p(a)}{q(a)}, \quad B = \sum_a p(a) \sum_b p(b | a) \log \frac{p(b | a)}{q(b | a)}, \quad C = \sum_b p(b) \sum_c p(c | b) \log \frac{p(c | b)}{q(c | b)}.$$

5. **Recognize KL pieces and combine:**

$$D_{\text{KL}}(p \| q) = D_{\text{KL}}(p(A) \| q(A)) + \sum_a p(a) D_{\text{KL}}(p(B | a) \| q(B | a)) + \sum_b p(b) D_{\text{KL}}(p(C | b) \| q(C | b)).$$

Figure 5: KL divergence decomposition into local components for Bayesian networks.

used o3 and its mini variant (OpenAI 2025), versions “o3-2025-04-16” and “o3-mini-2025-01-31”, and DeepSeek-R1 (DeepSeek-AI et al. 2025a), version “DeepSeek-R1-0528”. All models were interfaced using the LangChain framework (Chase 2022), ensuring consistent interaction.

LLMs’ Hyper-Parameters

A “temperature” of 0.1 was utilized to maintain minimal stochasticity in outputs. For reasoning models, the “reasoning effort” was set to *medium*. We initially explored the impact of sampling by performing up to five repeated samples per inference. However, we found that multiple samples did not meaningfully affect aggregate outcomes across the evaluated set of 80 Bayesian Networks, likely due to the low temperature setting. Consequently, given the number of LLMs and the dataset size, all subsequent experiments used a single sample to control cost. Output lengths were not constrained, allowing the models to elaborate their reasoning freely. In instances where models produced responses that deviated from the required format or where output text generation was interrupted midway, additional prompts were provided until valid responses were obtained.

EDP’s Hyper-Parameters

In our EDP formula, we have to select the hyper-parameter, α , in the following formula:

$$p_i = \frac{\alpha q_i + c_i}{\alpha + \sum_{j=1}^m c_j}, \quad i = 1, \dots, m.$$

where q_i is the prior probability (from the LLM) and c_i is the observed count for state i . Ideally, α is selected by testing various α values on a dev dataset of a downstream task. In our EDP experiments, where we are not testing a downstream task, we use a heuristic to select the α . It is intuitive that as the number of data samples increases, the importance of priors decreases. As a result, we set α to be proportional to the inverse of the number of data samples.

For classification experiments using EDP, for a dataset with N data samples, we set $\alpha = 0.5 \times N$ in the full-data regime. In the low-data regime, we select the optimal α from $0.5 \times N, 1.0 \times N, 2.0 \times N$ using the remaining training data as a development set.

LLMs’ Prompting Structure

Figure 6 shows the exact prompt we use to query the LLMs. All templates begin with a compact list of node names and natural-language descriptions (including each node’s state space) and then pose a probabilistic query conditioned on a specific parent configuration. For SepState, as shown in the top panel, for each state of the node, the model is asked a single question and instructed to provide a probability. We parse the trailing numeric value and repeat this for all states. For FullDist, as shown in the middle panel, the query requests the entire distribution in one response and explicitly supplies the order of states. We parse the tuple in the given order. For token probability, as shown in the bottom panel, the LLM is asked for only the most probable state name without any extra text. From the returned token scores for

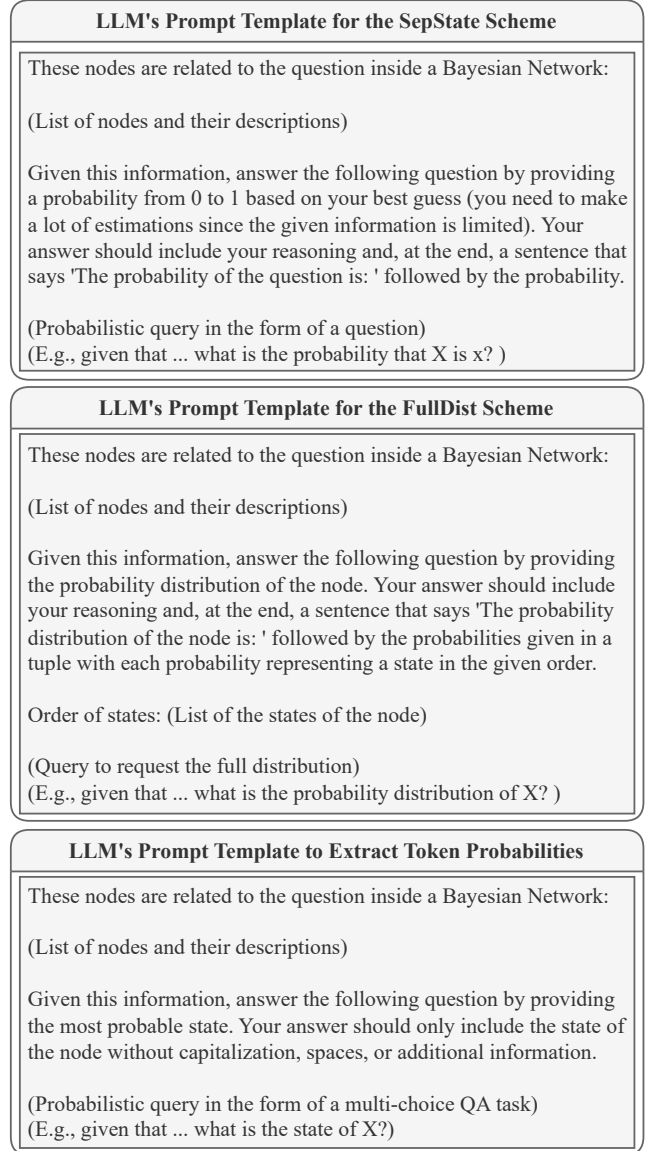


Figure 6: Prompt templates used for eliciting probabilistic responses from LLMs. The prompting structures for SepState, FullDist, and Extracting token probabilities are shown in the top, middle, and bottom panels, respectively.

each candidate string, we compute the probabilities of the states of the nodes. If a node’s state is not among the 20 returned candidate strings, we assign it a probability of 0. This occurs in only 12% of cases for GPT-4o and GPT-4o-mini. In our experiments, the probabilities of the returned strings typically sum to approximately 99%, justifying our assumption of a 0% probability for the absent states.

D Additional Experiments

EDP’s Impact on Downstream Tasks

Table 2 expands the classification study described in the main text by reporting additional results for DeepSeek-V3 and showing the variance in the results obtained in multiple runs. In the low-resource settings, the training cases are sampled from the training split, and results are averaged over five random runs. The \pm values in the 20 and 10 sample columns denote the empirical standard deviation across the five runs. For the LLM-only reference column, we use SepState with GPT-4o and FullDist with DeepSeek-V3. The corresponding EDP columns use the same extraction scheme as their LLM prior. These detailed results, which include DeepSeek-V3 in addition to GPT-4o, support the claims made in the main text: across both structures and most datasets, EDP matches or improves upon MLE, with the largest gains in the low-resource regimes.

EDP with Other LLMs and Sampling Methods

In this paper, we demonstrated that EDP improves probability estimates as measured by KL divergence, using GPT-4o. However, this trend is consistent across other LLMs as well. Figures 7, 8, and 9 illustrate EDP’s results for DeepSeek-V3, Gemini-pro 1.5, and Claude 3.5 Sonnet, respectively.

In our main experiments, we performed forward sampling on the entire BN. However, EDP consistently improves results under alternative sampling methods. Figure 10 shows EDP’s performance when sampling # data points per CPT row. Similarly, Figure 11 presents the results when using a related sampling strategy, where each CPT row is sampled $\# \times n$ times, with n representing the number of states of the node. These results prove that EDP’s improvements are independent of the sampling method.

SepState and FullDist with CPT KL Divergence

Figure 12 reports CPT KL for the methods discussed in the main paper. Consistent with the BN KL divergence, we observe that the relative ordering of methods is unchanged, meaning that the SepState performs the best among all baselines. Here, however, FullDist performs worse than the Uniform baseline in most LLMs.

E Varying Number of Parents and States

Figures 13 through 17 illustrate the CPT KL divergence for nodes with 2 to 6 states, respectively. Figures 18 through 25 depict the CPT KL divergence for nodes with 0 to 7 parents, respectively. These figures help to show the points made in the discussion section about the capability of LLMs in handling nodes with various state sizes and parents.

GPT-4o														
Dataset	Hill Climbing							Naïve Bayes						
		Full Data		20 Samples		10 Samples			Full Data		20 Samples		10 Samples	
	SepState	MLE	EDP	MLE	EDP	MLE	EDP	SepState	MLE	EDP	MLE	EDP	MLE	EDP
HV84*	.24	.94	.91	.87±.05	.80±.16	.78±.10	.85 ±.13	.40	.94	.91	.92 ±.01	.90±.02	.91 ±.02	.87±.01
PhDA*	.41	.38	.41	.35±.05	.41 ±.00	.34±.04	.41 ±.01	.45	.44	.44	.36±.03	.41 ±.01	.34±.04	.41 ±.03
Pokemon	.23	.62	.62	.62 ±.00	.62 ±.00	.54 ±.12	.54 ±.17	.48	.62	.60	.59±.05	.60 ±.01	.53±.04	.54 ±.08
Titanic	.42	.42	.42	.42 ±.00	.42 ±.00	.42 ±.00	.42 ±.00	.57	.11	.55	.22±.14	.57 ±.00	.42±.15	.56 ±.01
CAD1	.87	.83	.83	.74±.05	.85 ±.02	.63±.08	.84 ±.04	.77	.81	.85	.83±.04	.86 ±.03	.80±.06	.84 ±.05
CAD2	.76	.65	.76	.76 ±.00	.76 ±.00	.60±.14	.76 ±.00	.50	.86	.79	.73±.08	.78 ±.03	.77±.10	.78 ±.06
Covid	.74	.71	.73	.70±.03	.72 ±.01	.72 ±.01	.72 ±.00	.72	.71	.72	.71±.00	.72 ±.01	.69±.03	.72 ±.00
Puffin	.63	1.0	.93	.99 ±.03	.91±.03	.97 ±.04	.91±.03	.78	.93	.85	.90 ±.07	.88±.07	.87±.06	.88 ±.04
Traject*	.87	.87	.87	.75±.06	.86 ±.01	.68±.07	.86 ±.01	.80	.87	.87	.86 ±.00	.86 ±.01	.85±.03	.86 ±.02
Average	.57	.71	.72	.69±.03	.71 ±.03	.63±.07	.70 ±.05	.61	.70	.73	.68±.05	.73 ±.02	.69±.06	.72 ±.03

DeepSeek-V3														
Dataset	Hill Climbing							Naïve Bayes						
		Full Data		20 Samples		10 Samples			Full Data		20 Samples		10 Samples	
	FullDist	MLE	EDP	MLE	EDP	MLE	EDP	FullDist	MLE	EDP	MLE	EDP	MLE	EDP
HV84*	.93	.94	.93	.87±.06	.94 ±.03	.79±.11	.92 ±.00	.51	.94	.92	.92 ±.01	.88±.02	.91 ±.02	.89±.01
PhDA*	.38	.38	.38	.35±.05	.38 ±.00	.34±.04	.38 ±.00	.34	.44	.41	.36±.03	.40 ±.03	.34±.04	.40 ±.05
Pokemon	.62	.62	.62	.62 ±.00	.59±.08	.54±.12	.59 ±.08	.43	.62	.62	.59±.05	.61 ±.01	.53±.04	.59 ±.05
Titanic	.42	.42	.42	.42 ±.00	.42 ±.00	.42 ±.00	.42 ±.00	.57	.11	.57	.22±.14	.57 ±.00	.42±.15	.56 ±.01
CAD1	.89	.83	.88	.74±.05	.86 ±.04	.63±.08	.85 ±.03	.81	.81	.88	.83±.04	.85 ±.03	.80±.06	.83 ±.05
CAD2	.76	.65	.76	.57±.16	.76 ±.00	.57±.11	.76 ±.00	.33	.86	.79	.73 ±.08	.73 ±.12	.77±.10	.79 ±.00
Covid	.72	.71	.73	.70±.03	.71 ±.03	.72 ±.01	.70±.03	.72	.71	.73	.71±.00	.72 ±.01	.69±.03	.72 ±.00
Puffin	.33	1.0	.93	.99 ±.03	.93±.00	.97 ±.04	.91±.03	.48	.93	.85	.90 ±.07	.88±.07	.87 ±.06	.87 ±.06
Traject*	.59	.87	.87	.75±.06	.84 ±.03	.68±.07	.82 ±.03	.69	.87	.81	.86 ±.00	.82±.02	.85 ±.03	.82±.04
Average	.63	.71	.72	.67±.05	.71 ±.02	.63±.06	.71 ±.02	.54	.70	.73	.68±.05	.72 ±.03	.69±.06	.72 ±.03

Table 2: Macro-F₁ classification scores on nine datasets for BN classifiers. Columns include three methods, *SepState* or *FullDist* using GPT-4o or DeepSeek-V3, *MLE*, and *EDP*, under two graph structures, HillClimbing and Naïve Bayes. Full Data uses the entire training split, whereas 20 and 10 Samples simulate low-resource regimes. Within each data regime, the higher of *MLE* vs. *EDP* is bolded. * datasets HV84, PhDA and Traject refer to HouseVote84, PhDArticles and Trajectories, respectively.

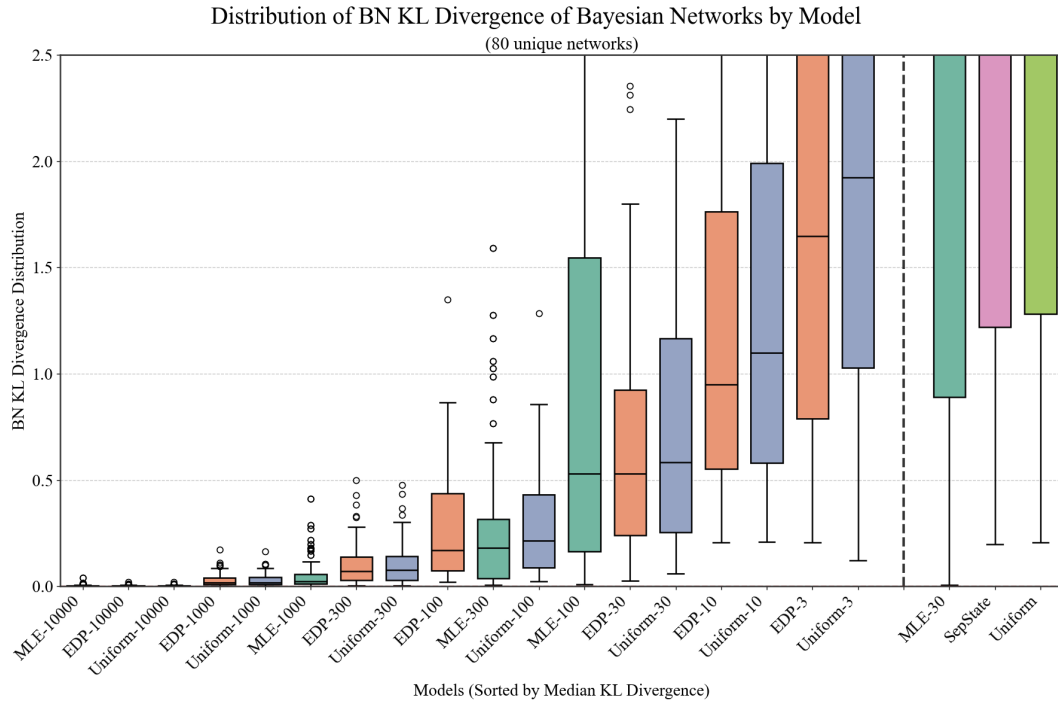


Figure 7: Boxplot of distribution of BN KL divergence over 80 networks, contrasting models with DeepSeek-V3 priors (EDP-#), uniform priors (Uniform-#), and data-only estimates (MLE-#). The numeral after the “-” denotes the sample size.

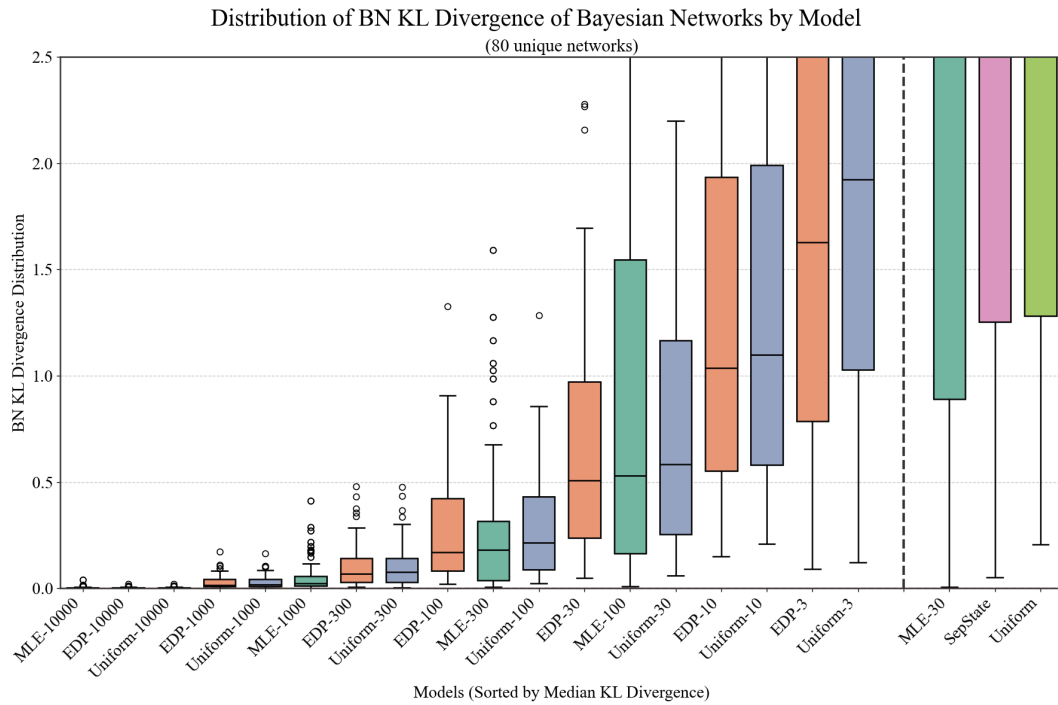


Figure 8: Boxplot of distribution of BN KL divergence over 80 networks, contrasting models with Gemini-pro 1.5 priors (EDP-#), uniform priors (Uniform-#), and data-only estimates (MLE-#). The numeral after the “-” denotes the sample size.

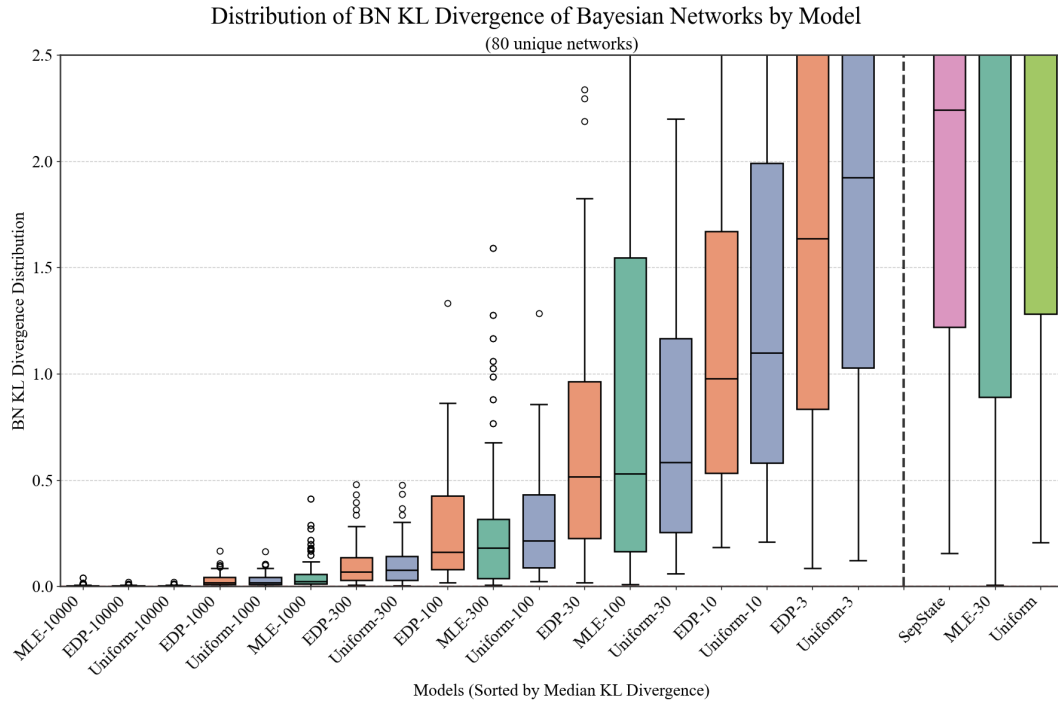


Figure 9: Boxplot of distribution of BN KL divergence over 80 networks, contrasting models with Claude 3.5 Sonnet priors (EDP-#), uniform priors (Uniform-#), and data-only estimates (MLE-#). The numeral after the “-” denotes the sample size.

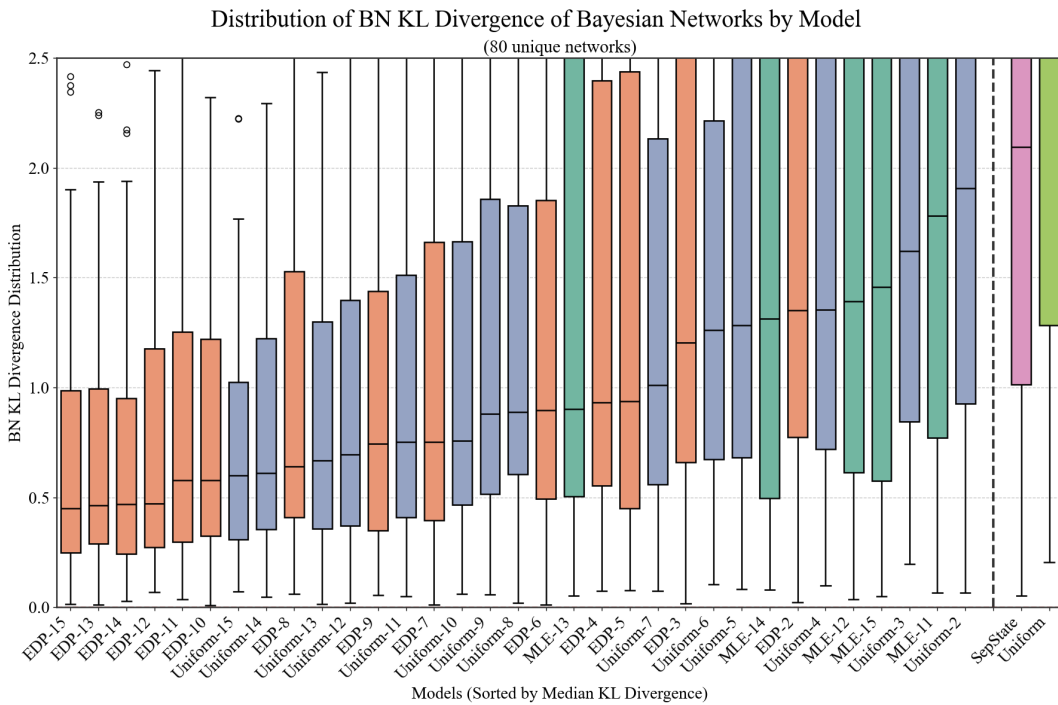


Figure 10: Boxplot of distribution of BN KL divergence over 80 networks, contrasting models with GPT-4o priors (EDP-#), uniform priors (Uniform-#), and data-only estimates (MLE-#). The numeral after the “-” denotes the sample size. In this figure, the data for each row of the CPT is sampled by # instances.

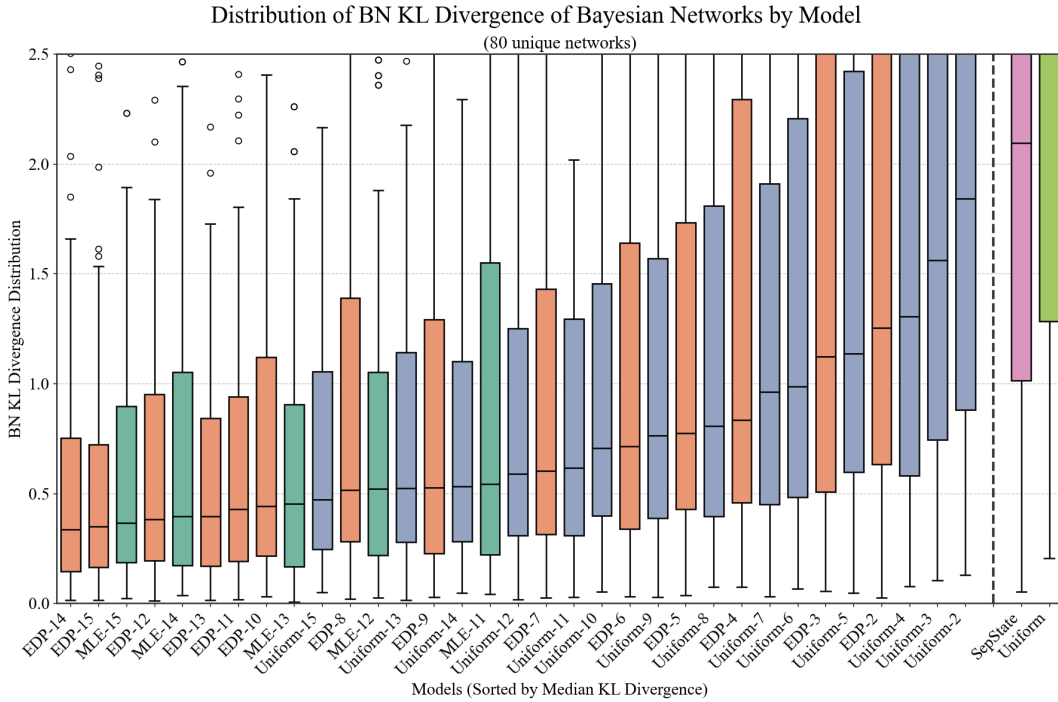


Figure 11: Boxplot of distribution of BN KL divergence over 80 networks, contrasting models with GPT-4o priors (EDP-#), uniform priors (Uniform-#), and data-only estimates (MLE-#). The numeral after the “-” denotes the sample size. In this figure, the data for each row of the CPT is sampled by $\# \times n$ times, with n representing the number of states of the node.

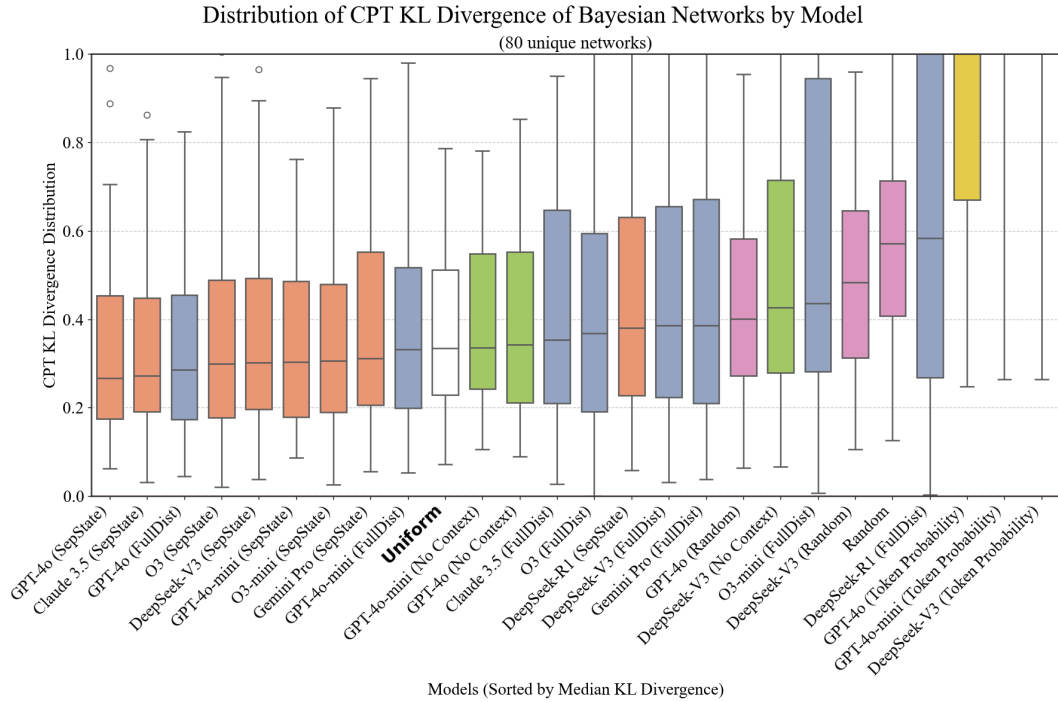


Figure 12: Boxplot showing the distribution of CPT KL divergence values across 80 unique BNs for various models, sorted by their median KL divergence. Lower values indicate better alignment with ground truth CPTs.

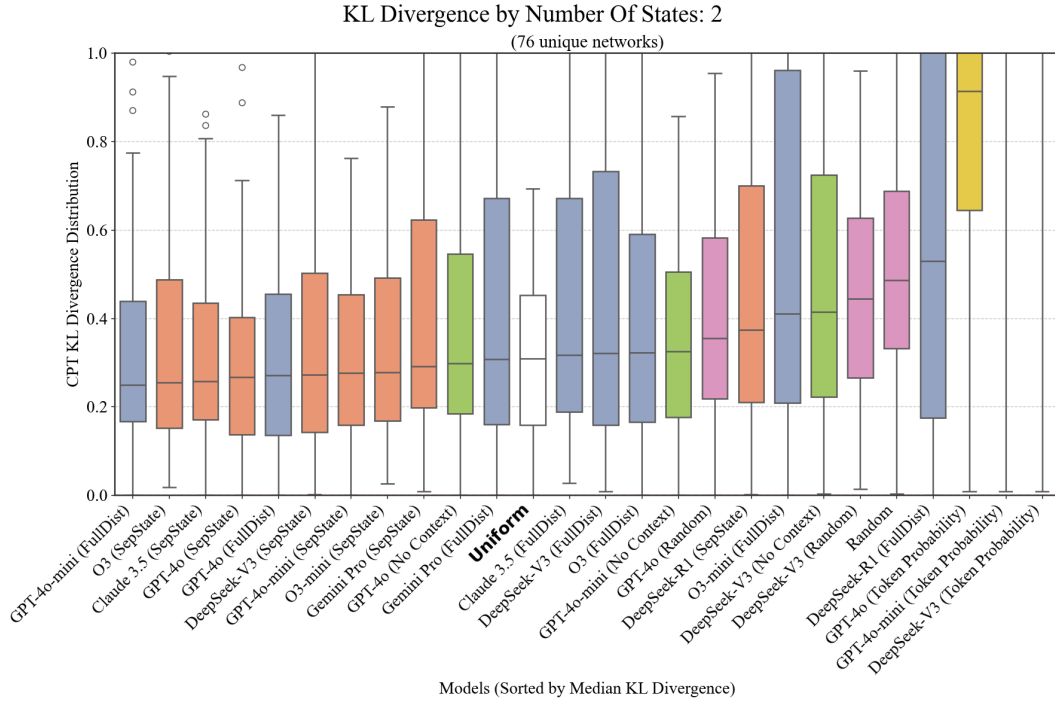


Figure 13: CPT KL divergence for nodes with 2 states.

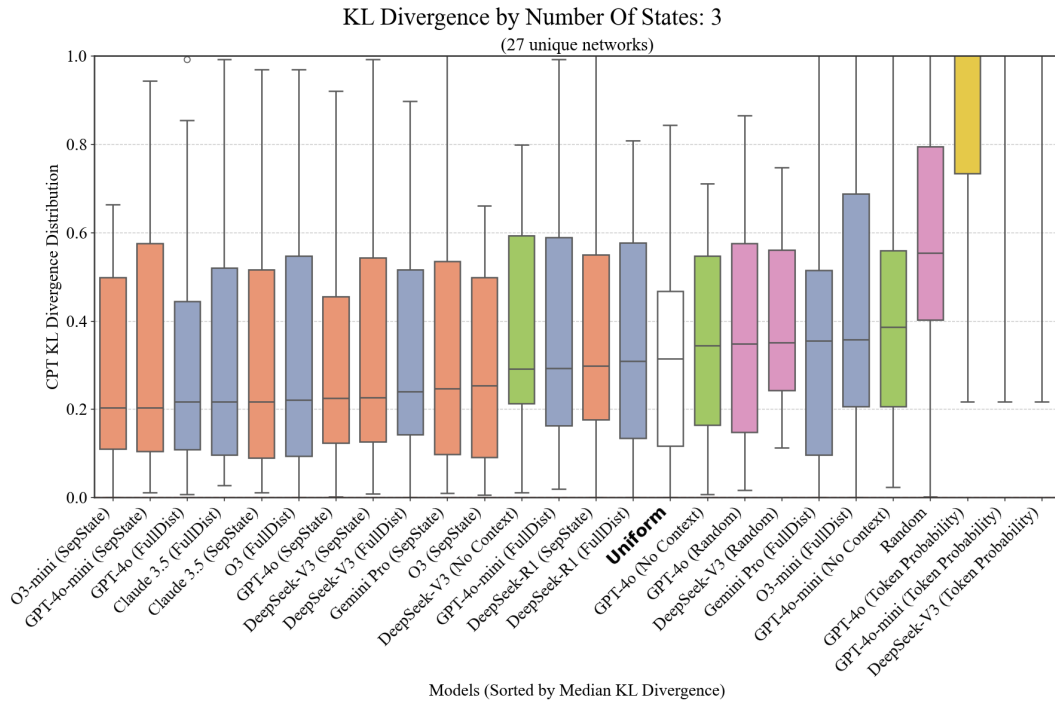


Figure 14: CPT KL divergence for nodes with 3 states.

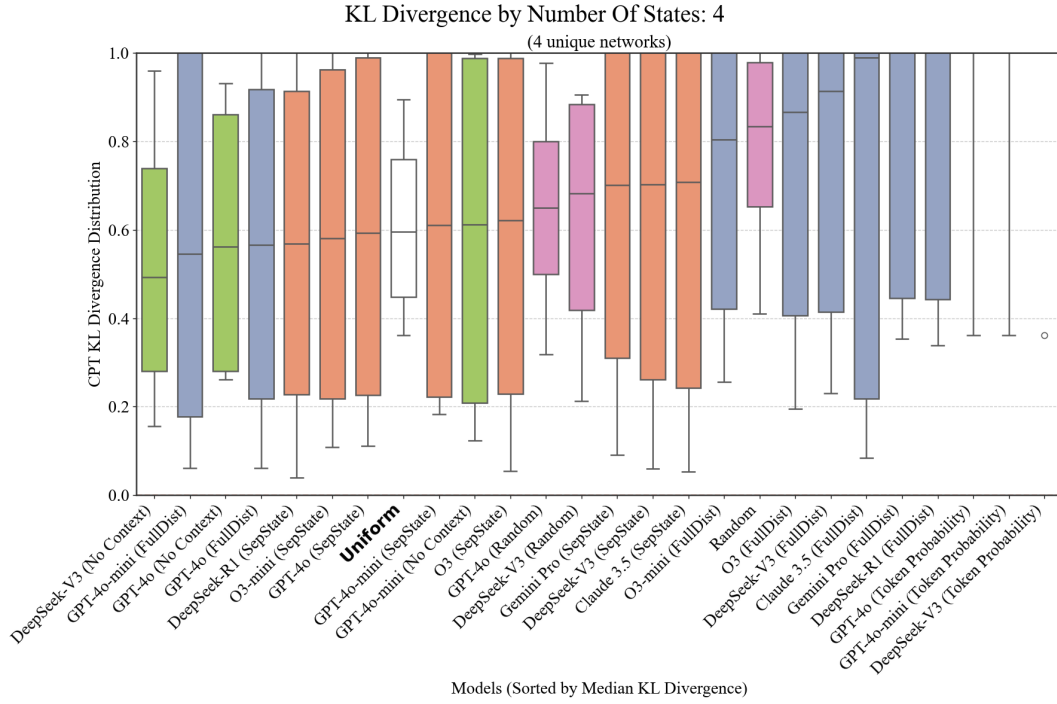


Figure 15: CPT KL divergence for nodes with 4 states.

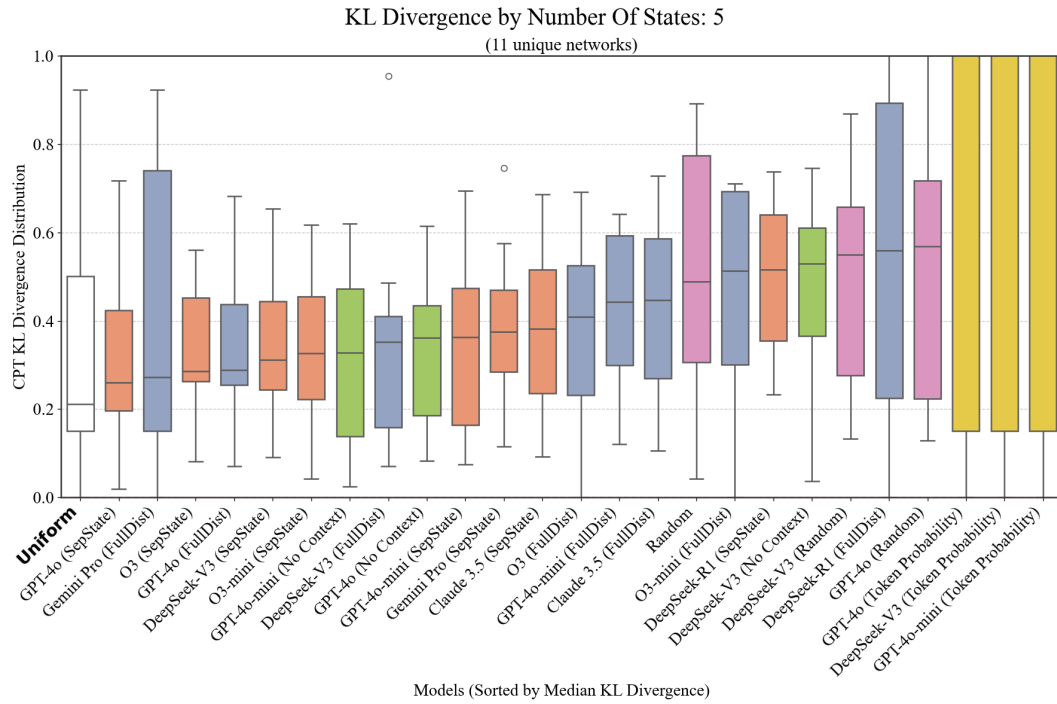


Figure 16: CPT KL divergence for nodes with 5 states.

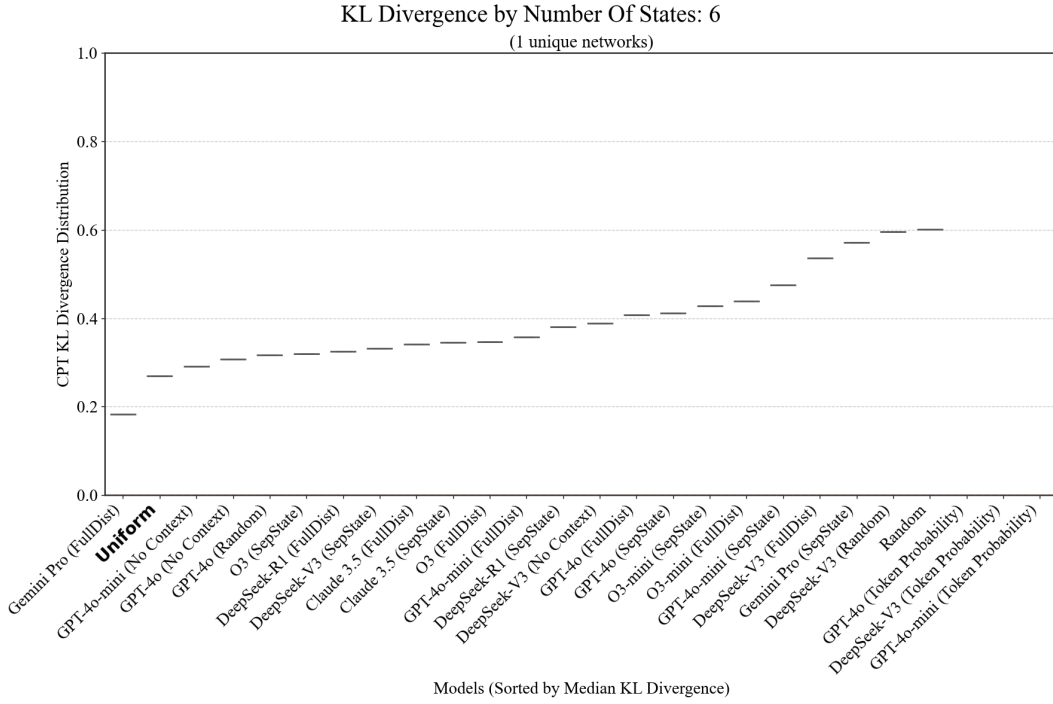


Figure 17: CPT KL divergence for nodes with 6 states.

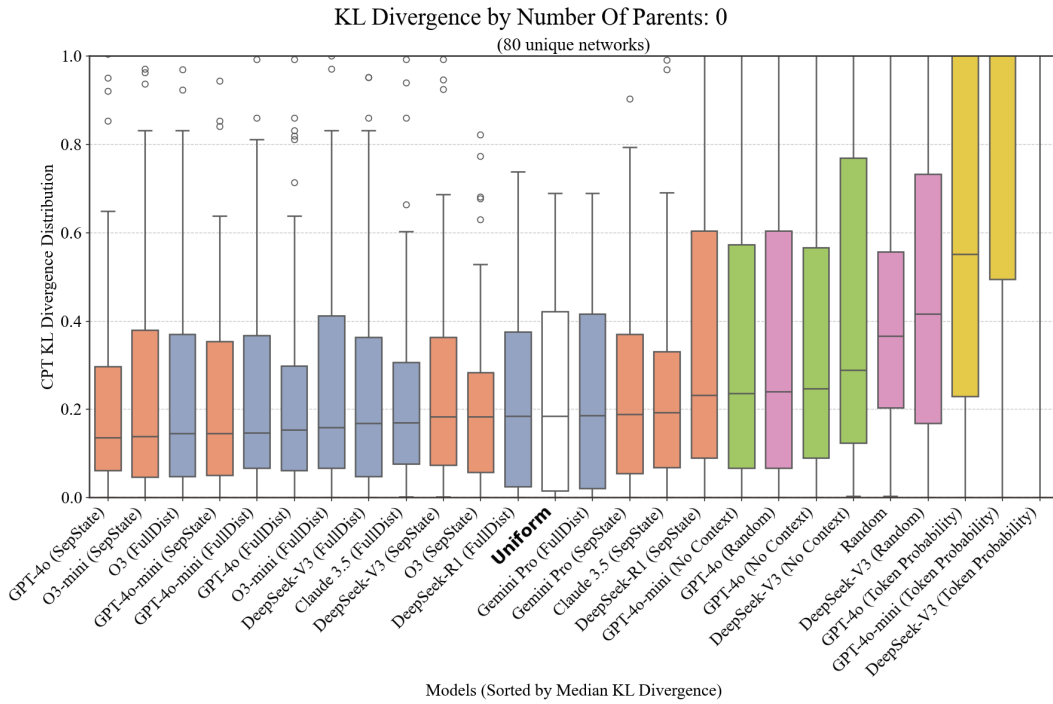


Figure 18: CPT KL divergence for nodes with 0 parents.

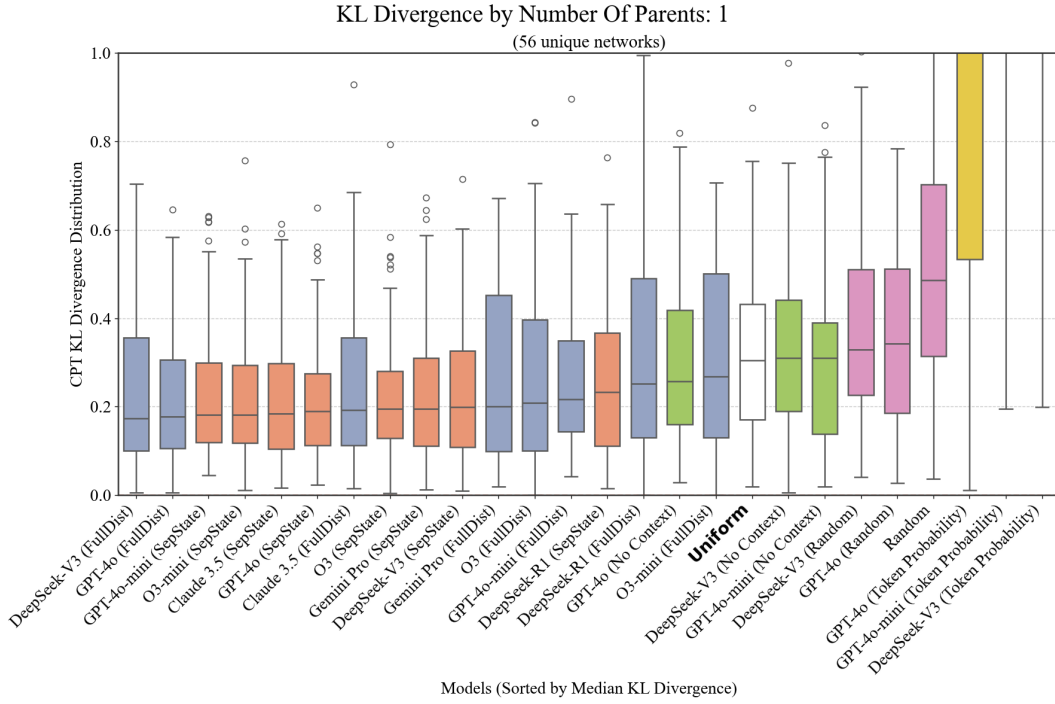


Figure 19: CPT KL divergence for nodes with 1 parents.

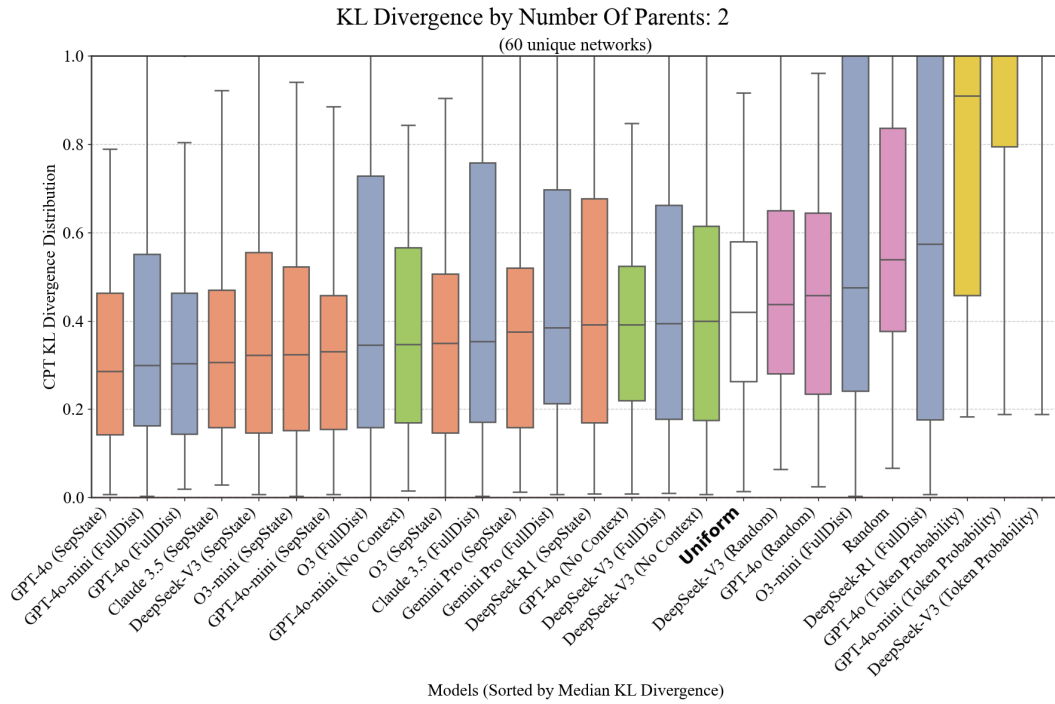


Figure 20: CPT KL divergence for nodes with 2 parents.

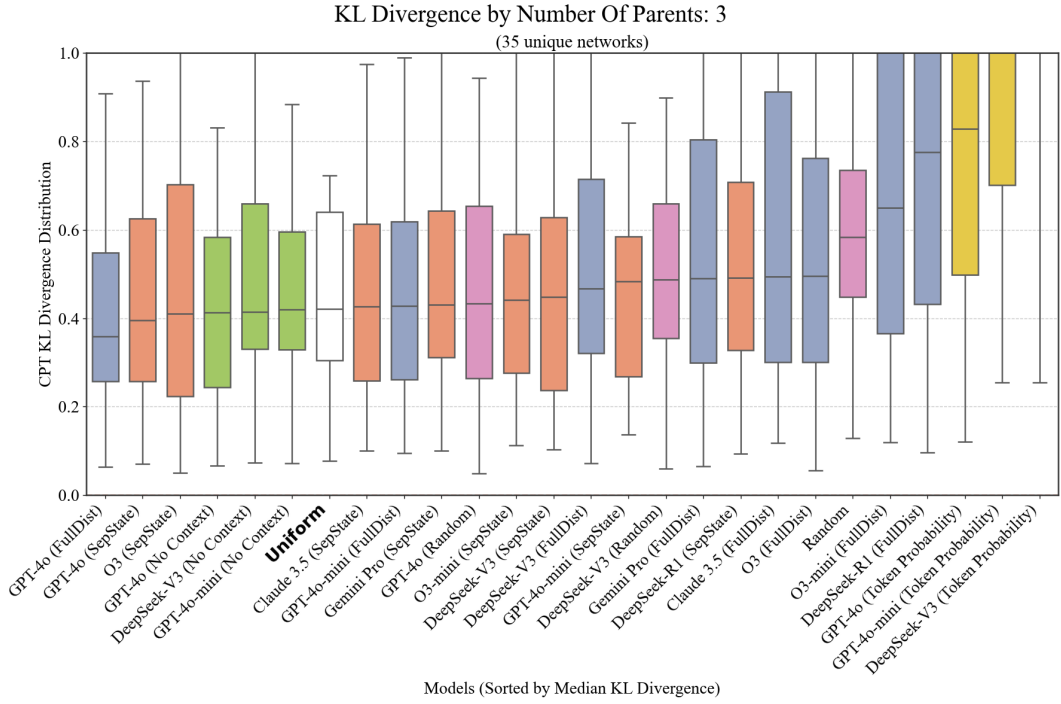


Figure 21: CPT KL divergence for nodes with 3 parents.

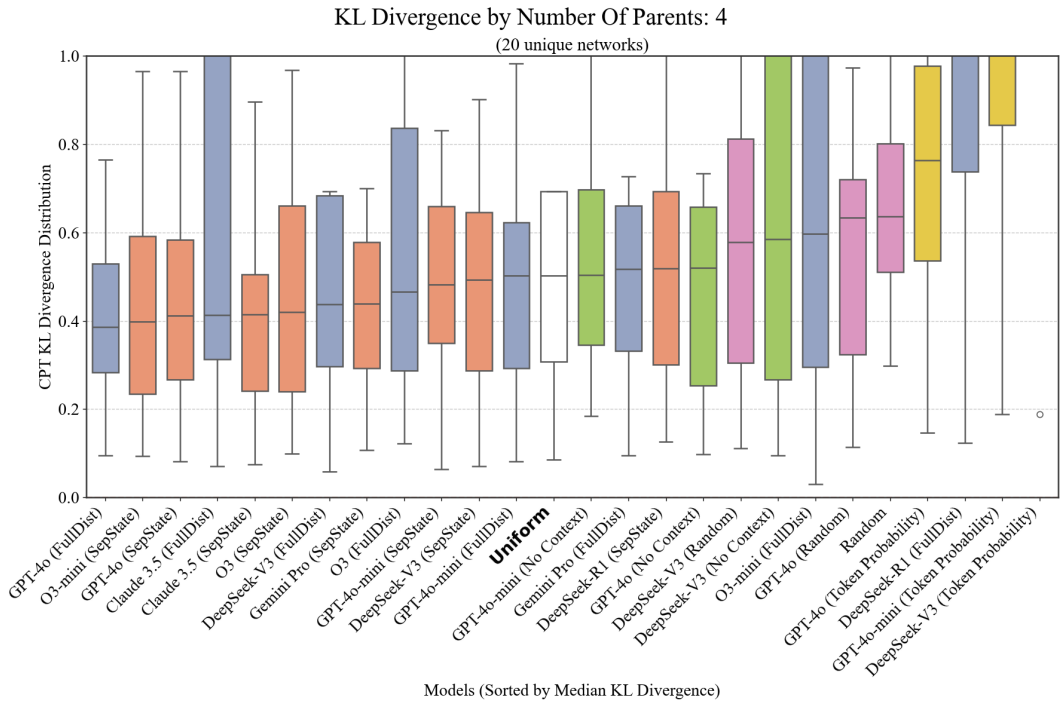


Figure 22: CPT KL divergence for nodes with 4 parents.

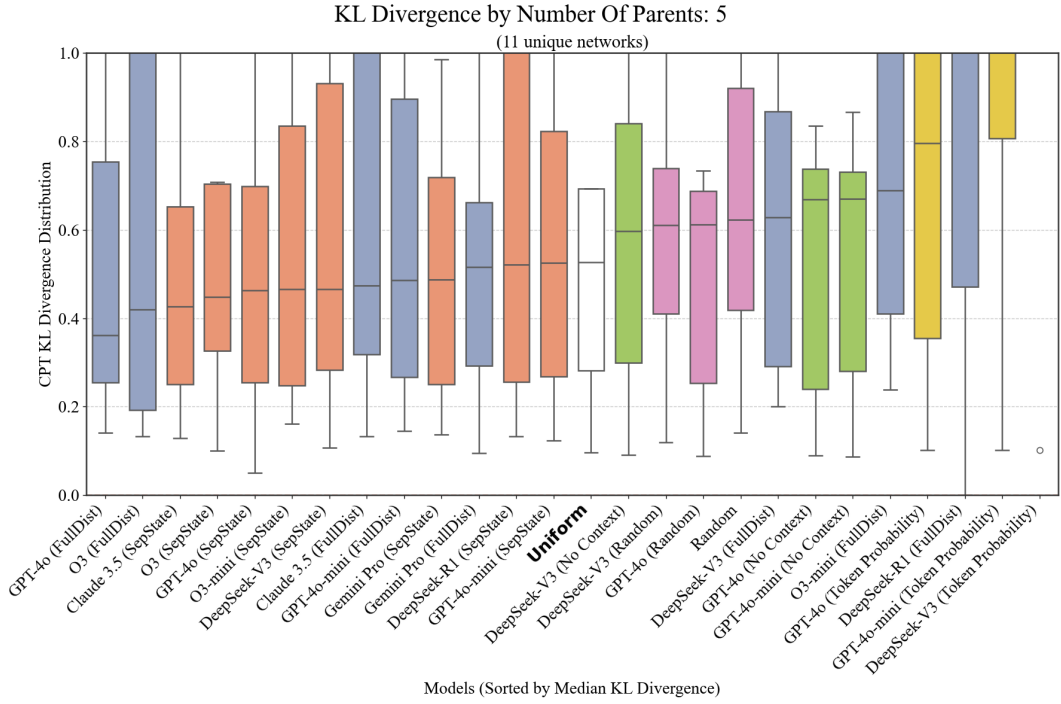


Figure 23: CPT KL divergence for nodes with 5 parents.

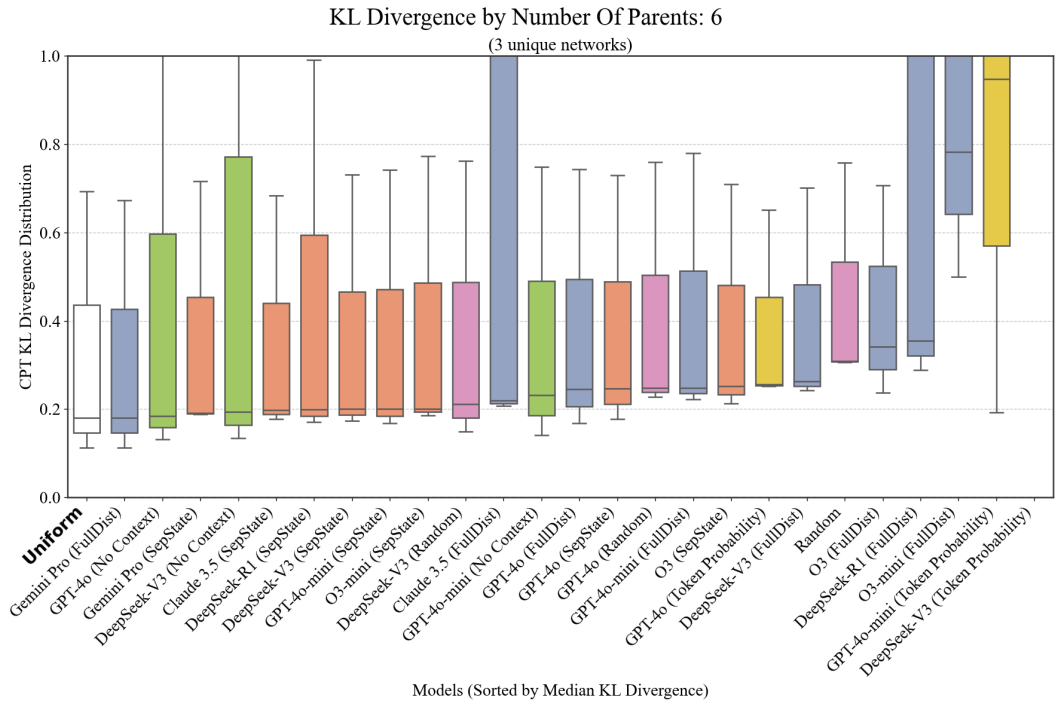


Figure 24: CPT KL divergence for nodes with 6 parents.

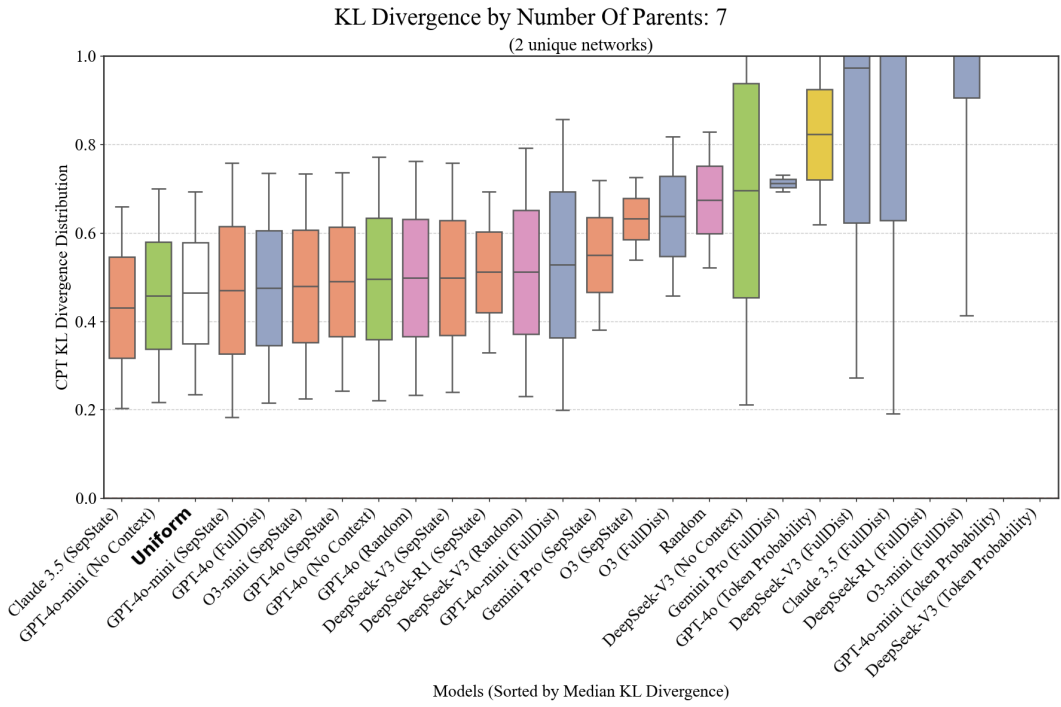


Figure 25: CPT KL divergence for nodes with 7 parents.